# MULTIVARIATE GEOMETRIC TAIL- AND RANGE-VALUE-AT-RISK

BY

KLAUS HERRMANN, MARIUS HOFERT AND MÉLINA MAILHOT

## ABSTRACT

A generalization of range-value-at-risk (RVaR) and tail-value-at-risk (TVaR) for $d$-dimensional distribution functions is introduced. Properties of these new risk measures are studied and illustrated. We provide special cases, applications and a comparison with traditional univariate and multivariate versions of the TVaR and RVaR.

## KEYWORDS

Multivariate risk measures, tail-value-at-risk, range-value-at-risk, geometric quantiles, dependence.

## 1. INTRODUCTION

Entities with several dependent portfolios, such as insurance companies and financial institutions, are allocating risk capital and comparing each business line and each single risk. These amounts are generally calculated using a risk decomposition technique which is applied to a total aggregate amount. The latter is usually obtained by means of a risk measure applied to an aggregate portfolio. To this end, risk measures are applied to the sum of all risks (thus considering their dependence) but without considering that some clusters of homogeneous risks might exist, which would be beneficial from a modeling perspective and which would provide more accurate results once risk measures are applied to the portfolio.

Top-down risk decomposition approaches consist of finding the total risk capital which must be allocated to the aggregate portfolio, traditionally based on a univariate risk measure applied to the aggregate portfolio, assuming that risks can all be pooled and mitigate one another. Then, from that amount, the split of capital to each component is conducted. The Euler principle, see McNeil *et al.* (2015), is an example of such a risk decomposition technique, which assumes a total portfolio composed of a linear combination of risks.

*Astin Bulletin* 50(1), 265-292. doi:10.1017/asb.2019.31 © 2019 by Astin Bulletin. All rights reserved.

https://doi.org/10.1017/asb.2019.31 Published online by Cambridge University Press

Bottom-up approaches use the amount allocated to each individual risk to built the total amount allocated to the portfolio. Factor-based and quantile approaches are examples of bottom-up approaches; see, for example, Rubin *et al.* (2009) and Kim and Hardy (2009) for more information of risk decomposition techniques, applied in an actuarial context.

The most influential regulatory frameworks in the insurance and finance industry, the Basel Accord and Solvency Directives, allow for flexibility when it comes to measuring risks, whether that is for comparison or capital allocation purposes. In the United States, Generally Accepted Accounting Principles are providing rules and guidelines in order to calculate capital allocation. In most other industrial countries, International Financial Reporting Standards are used for that same purpose. Internal models and measures are encouraged by regulators. Moreover, there is an increased interest toward multivariate risk measures, as have been presented and shown to be effective in providing a more representative share than risk decomposition techniques applied to univariate risk measures. A first application of level curves for risk management purposes has been presented in Cherubini *et al.* (2004). Then, Embrechts and Puccetti (2006) presented level sets, developed and redefined as multivariate lower and upper orthant VaR in Cossette *et al.* (2013). Based on this definition, Cossette *et al.* (2016) developed multivariate lower and upper orthant tail-value-at-risk. Di Bernardino *et al.* (2013), Di Bernardino *et al.* (2015) and Ben Tahar (2006) also presented different definitions of multivariate VaR and conditional tail expectation. More recently, Maume-Deschamps *et al.* (2017) presented a multivariate extension of expectiles, where the risk decomposition is embedded in the risk measure and the multivariate version of expectiles presented assumes risk mitigation throughout the portfolio, but allows for a multivariate model which presumably has a better fit for the considered data. Based on the multivariate geometric quantiles defined in Chaudhuri (1996), Herrmann *et al.* (2018) developed multivariate geometric expectiles. While univariate expectiles can be defined for random variables with finite first moment (see Newey and Powell, 1987), multivariate extensions are based on the existence of second moments (see Herrmann *et al.*, 2018; Maume-Deschamps *et al.*, 2017).

In this paper, we introduce multivariate geometric extensions of range-value-at-risk (RVaR) and TVaR. In the univariate case, RVaR is an attractive alternative to commonly used risk measures as it is robust, see Cont *et al.* (2010), and does not require moment restrictions. Contrary to multivariate expectiles, geometric RVaR overcomes the necessity to impose second moment conditions, which is relevant for heavy-tailed distributions. Moreover, compared to the alternative multivariate VaR and TVaR risk measures mentioned above, multivariate geometric risk measures allow for more flexibility as the customary univariate confidence levels are replaced with a multivariate index. This allows to assign an index to each (random) risk that is part of a portfolio. We also study properties of multivariate geometric RVaR and TVaR and provide several characteristics of these multivariate risk

https://doi.org/10.1017/asb.2019.31 Published online by Cambridge University Press

measures. Furthermore, we compare them and analyze their behavior under different dependence structures.

In Section 2, we present univariate VaR and multivariate geometric VaR and provide further insight into multivariate geometric quantiles. In Sections 3 and 4, multivariate geometric TVaR and RVaR are introduced and the choice of the multivariate index replacing the univariate confidence level is discussed. Section 5 is dedicated to studying the properties of these new multivariate geometric risk measures. Section 6 contains illustrations, special cases and examples of the multivariate geometric RVaR (and thus TVaR). Final conclusions are drawn in Section 7.

## 2. GEOMETRIC QUANTILES AND VALUE-AT-RISK

As an alternative to interpreting quantiles as the generalized inverse of the associated distribution function, quantiles can be obtained implicitly as minimizers of a suitable expected loss function. Denoting by $\rho_\alpha$ the *check function* (or *pinball*) loss

$$\rho_\alpha : \mathbb{R} \to [0, \infty), \quad \rho_\alpha(t) \mapsto \left|\alpha - \mathbb{1}_{(-\infty,0]}(t)\right| |t|, \tag{2.1}$$

the $\alpha$-quantile $F^{-1}(\alpha)$ of a distribution function $\boldsymbol{F}$ can be obtained as

$$F^{-1}(\alpha) = \underset{c\in\mathbb{R}}{\operatorname{argmin}}\, \mathbb{E}\left[\rho_\alpha(X - c)\right], \quad \alpha \in (0, 1). \tag{2.2}$$

This observation has opened up different branches of research: in a univariate context, Koenker and Bassett (1978) introduce quantile regression by introducing covariates into (2.2), while Newey and Powell (1987) define expectiles based on a modification of (2.1). By providing multivariate counterparts to (2.1) and (2.2), Chaudhuri (1996) introduces multivariate geometric quantiles.

In this paper, we focus on a related multivariate concept. In order to establish the notation we will use for the remainder of this article, we provide a streamlined introduction to multivariate geometric quantiles in the following paragraphs, but refer to Chaudhuri (1996), Girard and Stupfler (2015, 2017) and Herrmann *et al.* (2018) for a more detailed discussion. We denote by $\|\boldsymbol{x}\|_2 = \sqrt{\boldsymbol{x}^\top \boldsymbol{x}}$ and $\langle \boldsymbol{x}, \boldsymbol{y}\rangle = \boldsymbol{x}^\top \boldsymbol{y}$ the Euclidean norm and inner product of two vectors $\boldsymbol{x}, \boldsymbol{y} \in \mathbb{R}^d$. The open unit ball in $\mathbb{R}^d$ is denoted by $B^d = \{\boldsymbol{x} \in \mathbb{R}^d : \|\boldsymbol{x}\|_2 < 1\} \subset \mathbb{R}^d$. We generally consider a $d$-dimensional random vector $\boldsymbol{X} \in L^1(\Omega, \mathcal{F}, \mathbb{P})$ defined on the underlying probability space $(\Omega, \mathcal{F}, \mathbb{P})$ and a fixed index vector $\boldsymbol{\alpha} \in B^d$ generalizing the univariate confidence level. In analogy to the univariate case, the vector $\boldsymbol{\alpha} \in B^d$ is of dimension $d$, assigning a single index to each random variable. The corresponding multivariate geometric quantile, or multivariate geometric VaR, is defined as

$$\mathrm{VaR}_{\boldsymbol{\alpha}}(\boldsymbol{X}) = \underset{\boldsymbol{c}\in\mathbb{R}^d}{\operatorname{argmin}}\, \mathbb{E}\left[\Phi_{\boldsymbol{\alpha}}(\boldsymbol{X} - \boldsymbol{c})\right]. \tag{2.3}$$

https://doi.org/10.1017/asb.2019.31 Published online by Cambridge University Press

While (2.3) generalizes (2.2), the appropriate multivariate version $\Phi_{\boldsymbol{\alpha}}$ of the loss function $\rho_\alpha$ is defined by

$$\Phi_{\boldsymbol{\alpha}} : \mathbb{R}^d \to [0, \infty), \quad \boldsymbol{t} \mapsto \Phi_{\boldsymbol{\alpha}}(\boldsymbol{t}) = \frac{1}{2}(\|\boldsymbol{t}\|_2 + \langle \boldsymbol{\alpha}, \boldsymbol{t} \rangle), \quad \boldsymbol{\alpha} \in B^d. \tag{2.4}$$

As shown in Chaudhuri (1996), the right-hand side of (2.3) is always finite and the minimization is thus well posed; the resulting geometric VaR is the unique minimizer of (2.3). It is important to notice that the univariate version of geometric VaR implied by (2.3) is based on a confidence level $\alpha \in [-1, 1]$, instead of the traditional $\alpha \in [0, 1]$. The traditional confidence level in $[0, 1]$ can be recovered by an appropriate linear re-indexing; see Section 6.3 and also Herrmann *et al.* (2018) for an in-depth discussion. To clearly distinguish both concepts in the univariate setting, the standard quantiles with $\alpha \in [0, 1]$ are denoted by $F^{-1}$, while univariate geometric quantiles will be denoted by VaR. Denoting by $X$ a random variable with quantile function $F_X^{-1}$, we then have for $\alpha \in [0, 1]$ the connection

$$F_X^{-1}(\alpha) = \mathrm{VaR}_{(2\alpha-1)}(X).$$

Equation (2.3) can also be interpreted from the viewpoint of penalization. For $\boldsymbol{c} \in \mathbb{R}^d$, we denote by $P_{\boldsymbol{\alpha}}$ the function

$$P_{\boldsymbol{\alpha}}(\boldsymbol{c}; \boldsymbol{X}) = \sum_{i=1}^{d} \alpha_i \, (\mathbb{E}[X_i] - c_i),$$

for given weights $\alpha_i$ and finite expectations $\mathbb{E}[X_i]$. Combining (2.4) with the linearity of the expectation operator we find that

$$\mathrm{VaR}_{\boldsymbol{\alpha}}(\boldsymbol{X}) = \frac{1}{2} \operatorname*{argmin}_{\boldsymbol{c} \in \mathbb{R}^d} \quad \mathbb{E}[\|\boldsymbol{X} - \boldsymbol{c}\|_2] + P_{\boldsymbol{\alpha}}(\boldsymbol{c}; \boldsymbol{X}). \tag{2.5}$$

As noted by Chaudhuri (1996), for $\boldsymbol{\alpha} = \boldsymbol{0}$ the geometric VaR equals the spatial median; see Small (1990) for an overview on multivariate medians. The additional term in (2.5) can therefore be interpreted as a penalization term. When $\alpha_i \neq 0$, $P_{\boldsymbol{\alpha}}$ penalizes the difference between $\mathbb{E}[X_i]$ and $c_i$, and the geometric VaR is thus the penalized version of the spatial median. Likewise, the geometric expectiles of Herrmann *et al.* (2018) can be interpreted as penalized versions of the component-wise mean.

In comparison to other generalizations of quantiles to $d > 1$, geometric VaR has a number of attractive properties; see Theorem 2.1. While properties (1)–(3) are directly taken from Chaudhuri (1996), we prepare our discussion of (6) by providing a general proposition concerning properties of radially symmetric random vectors, including, for example, elliptical models as a special case.

https://doi.org/10.1017/asb.2019.31 Published online by Cambridge University Press

**Proposition 2.1 (Mean symmetry for minimal expected loss).** *Denote by* $\boldsymbol{X}$ *a radially symmetric random vector around* $\boldsymbol{\mu} \in \mathbb{R}^d$ *such that* $\boldsymbol{X} - \boldsymbol{\mu} \overset{d}{=} \boldsymbol{\mu} - \boldsymbol{X}$, *and by* $L$ *a loss function,* $L\colon \mathbb{R}^d \to [0, \infty)$. *For the minimizer of the expected loss* $\boldsymbol{v}(\boldsymbol{X}) = \operatorname{argmin}_{\boldsymbol{c}\in\mathbb{R}^d} \mathbb{E}\,[L(\boldsymbol{X} - \boldsymbol{c})]$, *we then have that*

$$\tfrac{1}{2}\,(\boldsymbol{v}(\boldsymbol{X}) - \boldsymbol{v}(-\boldsymbol{X})) = \boldsymbol{\mu}.$$

**Proof.** We first note that $\boldsymbol{v}$ is a translation invariant functional, that is, for a fixed $\boldsymbol{x} \in \mathbb{R}^d$ we have $\boldsymbol{v}(\boldsymbol{X} + \boldsymbol{x}) = \boldsymbol{v}(\boldsymbol{X}) + \boldsymbol{x}$. Furthermore, we have that

$$\begin{aligned}\mathbb{E}[L(-\boldsymbol{X} - (\boldsymbol{v}(\boldsymbol{X}) - 2\boldsymbol{\mu})] &= \mathbb{E}[L(-(\boldsymbol{X} - \boldsymbol{\mu}) - \boldsymbol{v}(\boldsymbol{X}) + \boldsymbol{\mu})] \\ &= \mathbb{E}[L(-(\boldsymbol{X} - \boldsymbol{\mu}) - \boldsymbol{v}(\boldsymbol{X} - \boldsymbol{\mu}))] \\ &= \mathbb{E}[L((\boldsymbol{X} - \boldsymbol{\mu}) - \boldsymbol{v}(\boldsymbol{X} - \boldsymbol{\mu}))],\end{aligned}$$

where the last equation follows from radial symmetry. The right-hand side is minimized by definition of $\boldsymbol{v}(\boldsymbol{X} - \boldsymbol{\mu})$. Therefore, the left-hand side is minimized leading to $\boldsymbol{v}(-\boldsymbol{X}) = \boldsymbol{v}(\boldsymbol{X}) - 2\boldsymbol{\mu}$. Rearranging terms then leads to the result. □

We can now go on to summarize properties of VaR in the following theorem.

**Theorem 2.1 (Properties of geometric** VaR**).** *Denote by* $\boldsymbol{X}, \boldsymbol{Y} \in L^1(\Omega, \mathcal{F}, \mathbb{P})$ *two* $d$*-dimensional random vectors and by* $\boldsymbol{\alpha} \in B^d$ *a fixed index vector. Then*

*(1)* $\mathrm{VaR}_{\boldsymbol{\alpha}}(\boldsymbol{X} + \boldsymbol{x}) = \mathrm{VaR}_{\boldsymbol{\alpha}}(\boldsymbol{X}) + \boldsymbol{x}$ *for any vector* $\boldsymbol{x} \in \mathbb{R}^d$ *(translation invariance),*

*(2)* $\mathrm{VaR}_{\boldsymbol{\alpha}}(\sigma \boldsymbol{X}) = \sigma\, \mathrm{VaR}_{\boldsymbol{\alpha}}(\boldsymbol{X})$ *for any scalar* $\sigma > 0$ *(positive homogeneity),*

*(3)* $\mathrm{VaR}_{A\boldsymbol{\alpha}}(A\boldsymbol{X}) = A\,\mathrm{VaR}_{\boldsymbol{\alpha}}(\boldsymbol{X})$ *for any orthogonal matrix* $A \in \mathbb{R}^{d\times d}$ *(rotation),*

*(4)* $\mathrm{VaR}_{\boldsymbol{\alpha}}(\boldsymbol{X}) = \mathrm{VaR}_{\boldsymbol{\alpha}}(\boldsymbol{Y})$ *for all* $\boldsymbol{\alpha} \in B^d$ *if and only if* $F_{\boldsymbol{X}} = F_{\boldsymbol{Y}}$ *for all* $\boldsymbol{x} \in \mathbb{R}^d$ *(distributional equality),*

*(5)* $\mathrm{VaR}_{\boldsymbol{\alpha}}(-\boldsymbol{X}) = -\,\mathrm{VaR}_{-\boldsymbol{\alpha}}(\boldsymbol{X})$ *(sign change) and*

*(6) if* $\boldsymbol{X}$ *is radially symmetric around* $\boldsymbol{\mu} \in \mathbb{R}^d$ *then* $\frac{1}{2}\big(\mathrm{VaR}_{\boldsymbol{\alpha}}(\boldsymbol{X}) + \mathrm{VaR}_{-\boldsymbol{\alpha}}(\boldsymbol{X})\big) = \boldsymbol{\mu}$ *(location symmetry).*

**Proof.** Properties (1)–(3) are established in Chaudhuri (1996), while (4) is derived in Koltchinskii (1997). Item (5) follows as a corollary from (3) when considering $A = -\boldsymbol{I}_d$ and $-\boldsymbol{\alpha}$. To establish (6), we combine (5) with Proposition 2.1 to obtain $\boldsymbol{\mu} = \frac{1}{2}(\mathrm{VaR}_{\boldsymbol{\alpha}}(\boldsymbol{X}) - \mathrm{VaR}_{\boldsymbol{\alpha}}(-\boldsymbol{X})) = \frac{1}{2}(\mathrm{VaR}_{\boldsymbol{\alpha}}(\boldsymbol{X}) + \mathrm{VaR}_{-\boldsymbol{\alpha}}(\boldsymbol{X}))$. □

Geometric VaR has also been studied from the viewpoint of multivariate extreme value theory in Girard and Stupfler (2015, 2017). Generally it holds that $\|\mathrm{VaR}_{\boldsymbol{\alpha}}(\boldsymbol{X})\|_2 \to \infty$ if $\|\boldsymbol{\alpha}\|_2 \to 1$, even if the support of $\boldsymbol{X}$ is bounded. Furthermore, $\mathrm{VaR}_{\boldsymbol{\alpha}}(\boldsymbol{X}) / \|\mathrm{VaR}_{\boldsymbol{\alpha}}(\boldsymbol{X})\|_2 \to \boldsymbol{\beta}$ when $\boldsymbol{\alpha} \to \boldsymbol{\beta}$, with $\|\boldsymbol{\beta}\|_2 = 1$. This shows that geometric VaR asymptotically shares the same direction as the

https://doi.org/10.1017/asb.2019.31 Published online by Cambridge University Press

index vector. Under integrability conditions on the second moment, see Girard and Stupfler (2015), the covariance matrix of $\boldsymbol{X}$ determines the magnitude of $\mathrm{VaR}_{\boldsymbol{\alpha}}(\boldsymbol{X})$ in an asymptotic sense. In case the integrability conditions fail, it is the index of multivariate regular variation of the density of $\boldsymbol{X}$ that governs the asymptotic behavior of $\mathrm{VaR}_{\boldsymbol{\alpha}}(\boldsymbol{X})$; see Girard and Stupfler (2017).

## 3. Multivariate geometric TVaR and RVaR

In this section, we provide multivariate definitions of TVaR and RVaR based on geometric VaR discussed in Section 2. In the univariate case, TVaR of a random variable $X\colon \Omega \to \mathbb{R}$ and a confidence level $\alpha \in (0,1)$ is defined as an appropriately weighted integral over sufficiently extreme scenarios, given by

$$\mathrm{TVaR}_\alpha(X) = \frac{1}{1-\alpha}\int_\alpha^1 F_X^{-1}(u)du; \tag{3.1}$$

see Kaas *et al.* (2008) or McNeil *et al.* (2015), amongst others. From a theoretical point of view, TVaR is an attractive choice among possible univariate risk measures, due to the fact that it is coherent in the sense of Artzner *et al.* (1999) and TVaR takes tail risk into account.

As defined in Cont *et al.* (2010), RVaR is obtained as a generalization of TVaR when considering two confidence levels $0 \leqslant \alpha_1 < \alpha_2 \leqslant 1$ leading to the definition

$$\mathrm{RVaR}_{\alpha_1,\alpha_2}(X) = \frac{1}{\alpha_2-\alpha_1}\int_{\alpha_1}^{\alpha_2} F_X^{-1}(u)du. \tag{3.2}$$

In contrast to TVaR, RVaR leads to a robust historical risk estimator. However, this advantage comes with the drawback that RVaR is not coherent; see Cont *et al.* (2010) for details.

An alternative representation of TVaR and RVaR can be given in terms of the conditional expectation of a uniformly distributed random variable $U \sim \mathcal{U}([0,1])$ with density $f_U(u) = \mathbb{1}_{[0,1]}(u)$ as

$$\begin{aligned}\mathbb{E}\left[F_X^{-1}(U) \mid U \in [\alpha_1,\alpha_2]\right] &= \frac{1}{\mathbb{P}[U \in [\alpha_1,\alpha_2]]}\int_{[\alpha_1,\alpha_2]} F_X^{-1}(u) f_U(u)du \\ &= \frac{1}{\alpha_2-\alpha_1}\int_{\alpha_1}^{\alpha_2} F_X^{-1}(u)du = \mathrm{RVaR}_{\alpha_1,\alpha_2}(X);\end{aligned} \tag{3.3}$$

clearly, TVaR is obtained in the same way when setting $\alpha_2 = 1$. Our extension of TVaR and RVaR to the multivariate setting is based on the conditional expectation in (3.3). Instead of conditioning on an interval $[\alpha_1,\alpha_2]$, however, we condition on a subset $D$ of the closed unit ball when $d > 1$.

To prepare our generalization, we first discuss the uniform distribution on the closed unit ball $\overline{B}^d = \{\boldsymbol{x} \in \mathbb{R}^d : \|\boldsymbol{x}\|_2 \leqslant 1\}$ based on the Euclidean norm $\|\boldsymbol{x}\|_2$. Following standard multivariate analysis, the volume of the $d$-dimensional unit ball is given by

https://doi.org/10.1017/asb.2019.31 Published online by Cambridge University Press

$$\lambda(\overline{B}^d) = \frac{\pi^{d/2}}{\Gamma(d/2+1)},$$

where $\Gamma(x)$ denotes the gamma function. We therefore define the uniform probability measure $\mu$ on $\overline{B}^d$ by normalizing the Lebesgue measure $\lambda$, that is, for every Borel measurable subset $D \subseteq \overline{B}^d$ we set

$$\mu(D) = \frac{\lambda(D)}{\lambda(\overline{B}^d)} = \frac{\Gamma(d/2+1)}{\pi^{d/2}}\lambda(D).$$

The density of $\mu$ with respect to $\lambda$ is consequently given by the constant

$$f_\mu : \mathbb{R}^d \to [0,\infty), \boldsymbol{u} \mapsto f_\mu(\boldsymbol{u}) = \frac{\Gamma(d/2+1)}{\pi^{d/2}}\mathbb{1}_{\overline{B}^d}(\boldsymbol{u}).$$

Here, $\mathbb{1}_{\overline{B}^d}$ denotes the indicator function of the set $\overline{B}^d$, that is, $\mathbb{1}_{\overline{B}^d}(\boldsymbol{u}) = 1$ if $\boldsymbol{u} \in \overline{B}^d$, and zero otherwise. We are now prepared to establish the definition of geometric RVaR.

**Definition 3.1 (Geometric** RVaR**).** *Denote by* $\boldsymbol{U}$ *a random vector uniformly distributed on* $B^d$. *The* geometric range-value-at-risk $\mathrm{GRVaR}_D(\boldsymbol{X})$ *of a* $d$*-dimensional random vector* $\boldsymbol{X}$ *based on a measurable set of index vectors* $D \subseteq \overline{B}^d$ *with* $\mu(D) > 0$ *is defined as*

$$\mathrm{GRVaR}_D(\boldsymbol{X}) = \mathbb{E}[\mathrm{VaR}_U(\boldsymbol{X}) \mid \boldsymbol{U} \in D]. \tag{3.4}$$

Considering that TVaR is a special case of RVaR when $\alpha_2 = 1$ in the univariate case, it is appropriate to write $\mathrm{GTVaR}_D(\boldsymbol{X})$ instead of $\mathrm{GRVaR}_D(\boldsymbol{X})$ whenever $D$ extends to the boundary of $\overline{B}^d$. For absolutely continuous random variables in the univariate case, RVaR as defined in (3.3) can equivalently be formulated in an expected-shortfall-type fashion as $\mathrm{RVaR}_{\alpha_1,\alpha_2}(X) = \mathbb{E}\left[X | X \in \left[F_X^{-1}(\alpha_1), F_X^{-1}(\alpha_2)\right]\right]$, where $0 \leqslant \alpha_1 < \alpha_2 \leqslant 1$. While this opens the possibility for a multivariate generalization along the lines of Definition 3.1, we focus on the proposed generalization of TVaR and RVaR for the remainder of this article.

It will often be advantageous to rewrite (3.4) in terms of an integral. Comparable to the univariate case, GRVaR can be expressed by

$$\begin{aligned}\mathrm{GRVaR}_D(\boldsymbol{X}) &= \mathbb{E}[\mathrm{VaR}_U(\boldsymbol{X}) \mid \boldsymbol{U} \in D] = \frac{1}{\mu(D)}\int_D \mathrm{VaR}_{\boldsymbol{u}}(\boldsymbol{X})\mu(d\boldsymbol{u}) \\ &= \frac{1}{\mu(D)}\int_D \mathrm{VaR}_{\boldsymbol{u}}(\boldsymbol{X})\frac{\Gamma(d/2+1)}{\pi^{d/2}}\lambda(d\boldsymbol{u}) \\ &= \frac{\Gamma(d/2+1)}{\pi^{d/2}\mu(D)}\int_D \mathrm{VaR}_{\boldsymbol{u}}(\boldsymbol{X})\lambda(d\boldsymbol{u}),\end{aligned} \tag{3.5}$$

https://doi.org/10.1017/asb.2019.31 Published online by Cambridge University Press

where we understand that the integral over a vector of functions denotes component-wise integration.

Concerning the choice of the uniform distribution on $\overline{B}^d$, we remark that any distribution on $\overline{B}^d$ reducing to the uniform distribution on $[-1, 1]$ in the one-dimensional case could be used to provide a generalization of GRVaR in the spirit of Definition 3.1. We focus on the uniform distribution on $\overline{B}^d$ as it naturally generalizes the uniform distribution on $[-1, 1]$ and allows for an efficient Monte Carlo simulation of relevant subsets of $\overline{B}^d$; see Algorithm 6.1.

Just as in the case of the univariate version of geometric VaR, the univariate version of GRVaR following from our Definition 3.1 is based on confidence levels $\alpha_1, \alpha_2 \in [-1, 1]$ instead of the traditional $\alpha_1, \alpha_2 \in [0, 1]$ as in (3.2). As mentioned before, the traditional confidence levels in $[0, 1]$ can be recovered by an appropriate linear re-indexing.

## 4. Choice of index level sets

In the univariate case, the integration domain $[\alpha, 1)$ in case of TVaR or $[\alpha_1, \alpha_2]$ in case of RVaR is chosen to represent extreme quantiles of the underlying risk. In light of the multivariate framework in Definition 3.1, the integration domain now needs to be replaced with a subset of the closed unit ball $D \subseteq \overline{B}^d$ representing extreme quantiles for $d > 1$.

In pursuit of this effort, we introduce for $0 \leqslant \alpha_1 < \alpha_2 \leqslant 1$ the ring

$$D(\alpha_1, \alpha_2) = \{\boldsymbol{u} \in \mathbb{R}^d : \alpha_1 \leqslant \|\boldsymbol{u}\|_2 \leqslant \alpha_2\} \subseteq \overline{B}^d.$$

This set consists of all index vectors $\boldsymbol{\alpha} \in \overline{B}^d$ that can be used as a basis to compute $\mathrm{VaR}_{\boldsymbol{\alpha}}(\boldsymbol{X})$ and lead to high quantiles in this sense. For reference, we compute the measure of $D(\alpha_1, \alpha_2)$ under $\boldsymbol{\lambda}$ and $\mu$ as

$$\boldsymbol{\lambda}(D(\alpha_1, \alpha_2)) = \frac{\pi^{d/2}(\alpha_2^d - \alpha_1^d)}{\Gamma(d/2 + 1)} \quad \text{and} \quad \mu(D(\alpha_1, \alpha_2)) = \alpha_2^d - \alpha_1^d.$$

Given that the univariate TVaR and RVaR are typically defined as the integral over high confidence levels in one direction, that is, the integration is carried out over $[\alpha, 1)$ and not over $(0, 1 - \alpha] \cup [\alpha, 1)$, a suitable subset of $D(\alpha_1, \alpha_2)$ needs to be selected in order to arrive at an intuitive generalization. Compared to the univariate case, the multivariate setting offers more choice in the sense that high quantiles can, for example, be characterized by requiring all indices to be positive, that is, considering extreme outcomes in all variables, or by requiring at least one index to be positive, that is, considering outcomes that are extreme in at least one variable.

We establish two valid generalizations of the univariate case by intersecting $D(\alpha_1, \alpha_2)$ with the appropriate orthants (subsets of $\mathbb{R}^d$ that generalize quadrants

https://doi.org/10.1017/asb.2019.31 Published online by Cambridge University Press

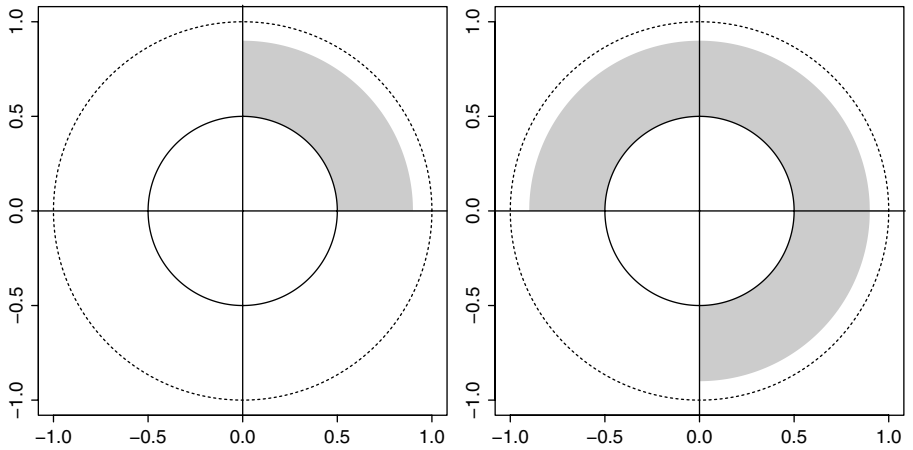



FIGURE 1: Integration domains $D_+(0.5, 0.9)$ (left, gray) and $D_-(0.5, 0.9)$ (right, gray) for $d = 2$. The set $D(0.5, 1)$ is indicated by the solid and dashed circles.

of $\mathbb{R}^2$ for dimensions $d > 2$). For a vector $\boldsymbol{s} \in \{-1, 1\}^d$, the corresponding orthant is defined as

$$O_{\boldsymbol{s}} = \{\boldsymbol{x} \in \mathbb{R}^d \mid s_i x_i \geqslant 0 \text{ for all } 1 \leqslant i \leqslant d\}. \tag{4.1}$$

We will define $O_+ = O_{\boldsymbol{s}_+}$ and $O_- = O_{\boldsymbol{s}_-}$ to denote the orthants based on $\boldsymbol{s}_+ = (1, \ldots, 1)$ and $\boldsymbol{s}_- = (-1, \ldots, -1)$. To capture high quantiles in all directions, it is therefore reasonable to consider the set $D_+(\alpha_1, \alpha_2) = D(\alpha_1, \alpha_2) \cap O_+$. High quantiles in at least one direction can be captured with $D_-(\alpha_1, \alpha_2) = D(\alpha_1, \alpha_2) \cap (\cup_{\boldsymbol{s} \in \{-1,1\}^d, \boldsymbol{s} \neq \boldsymbol{s}_-} O_{\boldsymbol{s}})$. By symmetry, it is clear that sets of the form $\overline{B}^d \cap O_{\boldsymbol{s}}$ all have the same $\mu$ measure, and that their measures sum up to one since they partition $\overline{B}^d$. We therefore have $\mu(\overline{B}^d \cap O_{\boldsymbol{s}}) = 2^{-d}$ for all $\boldsymbol{s} \in \{-1, 1\}^d$. As $D(\alpha_1, \alpha_2)$ is also symmetric, we get by the same argument

$$\mu(D_+(\alpha_1, \alpha_2)) = \frac{\alpha_2^d - \alpha_1^d}{2^d} \quad \text{and} \quad \mu(D_-(\alpha_1, \alpha_2)) = \frac{(2^d - 1)(\alpha_2^d - \alpha_1^d)}{2^d}. \tag{4.2}$$

We remark that in the univariate case $O_+ = O_- = [0, \infty)$ and therefore $D_+(\alpha_1, \alpha_2) = D_-(\alpha_1, \alpha_2) = [\alpha_1, \alpha_2]$. Taking $\Gamma(3/2) = \sqrt{\pi}/2$ into account, we recover the univariate Equations (3.1) and (3.2) for $\mathrm{GRVaR}_{D_+}(\boldsymbol{X})$ and $\mathrm{GRVaR}_{D_-}(\boldsymbol{X})$ based on (3.5).

For $d > 1$, the equality of $D_+$ and $D_-$ breaks down as can be seen from Figure 1, which shows the index vector sets $D_+(0.5, 0.9)$ and $D_-(0.5, 0.9)$ for $d = 2$.

Aside from specific choices of $D$, the general behavior of GRVaR with respect to $D$ is also of interest. As summarized in Girard and Stupfler (2017) and shown in Chaudhuri (1996) and Koltchinskii (1997), the mapping $\boldsymbol{\alpha} \mapsto \mathrm{VaR}_{\boldsymbol{\alpha}}(\boldsymbol{X})$ is one-to-one, continuous and has a continuous inverse. As such,

https://doi.org/10.1017/asb.2019.31 Published online by Cambridge University Press

basic topological properties of the index sets $D$ are preserved under the mapping. If $D$ is a closed set, then the image of $D$ under VaR is closed. The same preservation property also holds for open, (path-) connected and compact sets. Furthermore, sets $D_1$ and $D_2$ that are not intersecting are therefore also separated under the mapping $D \mapsto \mathrm{VaR}_D(\boldsymbol{X})$. In view of $D_+$ and $D_-$, this implies an order in the sense that the image of disjoint rings, for example, $D(\alpha_1, \alpha_2)$ and $D(\alpha_3, \alpha_4)$ for $0 \leqslant \alpha_1 < \alpha_2 < \alpha_3 < \alpha_4 \leqslant 1$, under VaR is forced further outwards from the center given by the spatial median $\mathrm{VaR}_{\mathbf{0}}(\boldsymbol{X})$ when $\alpha_2 \to 1$. In line with this observation, we have in general for a random vector $\boldsymbol{X}$ that $\|\mathrm{VaR}_{\boldsymbol{\alpha}}(\boldsymbol{X})\|_2 \to \infty$ if $\|\boldsymbol{\alpha}\|_2 \to 1$, as shown in Theorem 2.1 in Girard and Stupfler (2017). There is however no guarantee that the images of $D_+$ and $D_-$ under VaR stay ring shaped.

## 5. Properties of geometric RVaR

In this section, we set out to study the properties of GRVaR. We start by considering the impact of a nonrandom shift of the underlying random vector.

**Proposition 5.1 (Translation invariance).** *For a $d$-dimensional random vector $\boldsymbol{X}$ and $\boldsymbol{a} \in \mathbb{R}^d$, we have* $\mathrm{GRVaR}_D(\boldsymbol{X} + \boldsymbol{a}) = \mathrm{GRVaR}_D(\boldsymbol{X}) + \boldsymbol{a}$.

**Proof.** Component-wise integration leads to

$$\begin{aligned}
\mathrm{GRVaR}_D(\boldsymbol{X} + \boldsymbol{a}) &= \frac{\Gamma(d/2+1)}{\pi^{d/2}\mu(D)} \int_D \mathrm{VaR}_{\boldsymbol{u}}(\boldsymbol{X} + \boldsymbol{a}) \lambda(d\boldsymbol{u}) \\
&= \frac{\Gamma(d/2+1)}{\pi^{d/2}\mu(D)} \int_D (\mathrm{VaR}_{\boldsymbol{u}}(\boldsymbol{X}) + \boldsymbol{a}) \lambda(d\boldsymbol{u}) \\
&= \frac{\Gamma(d/2+1)}{\pi^{d/2}\mu(D)} \int_D \mathrm{VaR}_{\boldsymbol{u}}(\boldsymbol{X}) \lambda(d\boldsymbol{u}) + \frac{\Gamma(d/2+1)}{\pi^{d/2}\mu(D)} \int_D \boldsymbol{a} \lambda(d\boldsymbol{u}) \\
&= \frac{\Gamma(d/2+1)}{\pi^{d/2}\mu(D)} \int_D \mathrm{VaR}_{\boldsymbol{u}}(\boldsymbol{X}) \lambda(d\boldsymbol{u}) + \frac{\boldsymbol{a}}{\mu(D)} \int_D \mu(d\boldsymbol{u}) \\
&= \mathrm{GRVaR}_D(\boldsymbol{X}) + \boldsymbol{a}.
\end{aligned}$$

□

Following translation invariance, we next consider the impact of scaling. From a practical perspective, it is important to understand how GRVaR behaves when one, for example, changes the monetary unit.

**Proposition 5.2 (Positive homogeneity).** *For a $d$-dimensional random vector $\boldsymbol{X}$ and a positive scalar $\sigma > 0$, we have* $\mathrm{GRVaR}_D(\sigma \boldsymbol{X}) = \sigma\, \mathrm{GRVaR}_D(\boldsymbol{X})$.

https://doi.org/10.1017/asb.2019.31 Published online by Cambridge University Press

**Proof.** Via component-wise integration, we obtain that

$$\begin{aligned}\mathrm{GRVaR}_D(\sigma \boldsymbol{X}) &= \frac{\Gamma(d/2+1)}{\pi^{d/2}\mu(D)} \int_D \mathrm{VaR}_{\boldsymbol{u}}(\sigma \boldsymbol{X})\lambda(d\boldsymbol{u}) \\ &= \frac{\Gamma(d/2+1)}{\pi^{d/2}\mu(D)} \int_D \sigma\, \mathrm{VaR}_{\boldsymbol{u}}(\boldsymbol{X})\lambda(d\boldsymbol{u}) \\ &= \sigma \frac{\Gamma(d/2+1)}{\pi^{d/2}\mu(D)} \int_D \mathrm{VaR}_{\boldsymbol{u}}(\boldsymbol{X})\lambda(d\boldsymbol{u}) = \sigma\, \mathrm{GRVaR}_D(\boldsymbol{X}).\end{aligned}$$

□

In the following proposition, we study the impact of applying an orthogonal matrix to $\boldsymbol{X}$ and the underlying set of index vectors. As a special case, this operation encompasses a reordering of the entries of $\boldsymbol{X}$ or switching signs when going from losses to gains.

**Proposition 5.3 (Rotation).** *For a d-dimensional random vector $\boldsymbol{X}$ and an orthogonal matrix $A \in \mathbb{R}^{d\times d}$, we define the corresponding rotated integration domain by $\widetilde{D} = A[D] = \{A\boldsymbol{\alpha} \in \overline{B}^d : \boldsymbol{\alpha} \in D\} \subseteq \overline{B}^d$. Then we have that* $\mathrm{GRVaR}_{\widetilde{D}}(A\boldsymbol{X}) = A\,\mathrm{GRVaR}_D(\boldsymbol{X})$.

**Proof.** Due to the orthogonality of $A$, we have $|\det JL| = 1$, where $L(x) = Ax$ is the linear mapping connected to $A$ and $JL$ is the Jacobian matrix of first derivatives. This leads to

$$\begin{aligned}\int_{\widetilde{D}} \mathrm{VaR}_{\boldsymbol{v}}(A\boldsymbol{X})\lambda(d\boldsymbol{v}) &= \int_D \mathrm{VaR}_{A\boldsymbol{u}}(A\boldsymbol{X})\lambda(d\boldsymbol{u}) = \int_D A\,\mathrm{VaR}_{\boldsymbol{u}}(\boldsymbol{X})\lambda(d\boldsymbol{u}) \\ &= A\int_D \mathrm{VaR}_{\boldsymbol{u}}(\boldsymbol{X})\lambda(d\boldsymbol{u}),\end{aligned}$$

where we used the integral transformation theorem and the fact that $\mathrm{VaR}_{A\boldsymbol{u}}(A\boldsymbol{X}) = A\,\mathrm{VaR}_{\boldsymbol{u}}(\boldsymbol{X})$; see Theorem 2.1 (3). Including the normalizing constants in the integrals then gives the result. □

After we have established basic transformations in Propositions 5.1–5.3, we now turn to symmetry properties. For a given set of index vectors $D$, we denote by $-D = \{-\boldsymbol{\alpha} : \boldsymbol{\alpha} \in D\}$ the corresponding set with flipped signs. Based on the symmetry relations for VaR, we can recover a similar result for GRVaR.

**Corollary 5.1 (**GRVaR **vector sign symmetry).** *For a random vector $\boldsymbol{X}$, we have that*

$$\mathrm{GRVaR}_D(-\boldsymbol{X}) = -\,\mathrm{GRVaR}_{-D}(\boldsymbol{X}).$$

**Proof.** This follows from Proposition 5.3 with $A = -\boldsymbol{I}_d$ and a starting index set $-D$. □

https://doi.org/10.1017/asb.2019.31 Published online by Cambridge University Press

In case the underlying random vector $\boldsymbol{X}$ is radially symmetric, it is possible to establish symmetry of GRVaR similar to Theorem 2.1 in case of geometric VaR.

**Proposition 5.4 (**GRVaR **location symmetry).** *For a random vector $\boldsymbol{X}$ radially symmetric around $\boldsymbol{\mu}$ and a set of index vectors $D$, we have that*

$$\tfrac{1}{2}\left(\mathrm{GRVaR}_D(\boldsymbol{X}) + \mathrm{GRVaR}_{-D}(\boldsymbol{X})\right) = \boldsymbol{\mu}.$$

**Proof.** Combining Theorem 2.1 (5) and an integral transformation with $\phi(\boldsymbol{x}) = -\boldsymbol{x}$ as in Proposition 5.1, we have that

$$\begin{aligned}
\mathrm{GRVaR}_D(\boldsymbol{X}) &= \frac{\Gamma(d/2+1)}{\pi^{d/2}\mu(D)} \int_D \mathrm{VaR}_{\boldsymbol{u}}(\boldsymbol{X})\boldsymbol{\lambda}(d\boldsymbol{u}) \\
&= \frac{\Gamma(d/2+1)}{\pi^{d/2}\mu(D)} \int_D 2\boldsymbol{\mu} - \mathrm{VaR}_{-\boldsymbol{u}}(\boldsymbol{X})\boldsymbol{\lambda}(d\boldsymbol{u}) \\
&= \frac{\Gamma(d/2+1)}{\pi^{d/2}\mu(D)} \int_D 2\boldsymbol{\mu}\boldsymbol{\lambda}(d\boldsymbol{u}) - \frac{\Gamma(d/2+1)}{\pi^{d/2}\mu(D)} \int_D \mathrm{VaR}_{-\boldsymbol{u}}(\boldsymbol{X})\boldsymbol{\lambda}(d\boldsymbol{u}) \\
&= 2\boldsymbol{\mu} - \mathrm{GRVaR}_{-D}(\boldsymbol{X}),
\end{aligned}$$

from which the result follows by rearranging the terms. □

Just as the geometric VaR, GRVaR also uniquely identifies the underlying distribution function as shown in the following proposition.

**Proposition 5.5.** *For two random vectors $\boldsymbol{X}$ and $\boldsymbol{Y}$, we have* $\mathrm{GRVaR}_D(\boldsymbol{X}) = \mathrm{GRVaR}_D(\boldsymbol{Y})$ *for all measurable subsets $D \subseteq B^d$ if and only if $\boldsymbol{F}_X(\boldsymbol{x}) = \boldsymbol{F}_Y(\boldsymbol{x})$ for all $\boldsymbol{x} \in \mathbb{R}^d$.*

**Proof.** If $\boldsymbol{F}_X = \boldsymbol{F}_Y$, we immediately have $\mathrm{VaR}_{\boldsymbol{u}}(\boldsymbol{X}) = \mathrm{VaR}_{\boldsymbol{u}}(\boldsymbol{Y})$ for all $\boldsymbol{u} \in B^d$ and hence $\mathrm{GRVaR}_D(\boldsymbol{X}) = \mathrm{GRVaR}_D(\boldsymbol{Y})$ for every measurable $D \subseteq B^d$. For the other implication denote by $\mathscr{B}\left(B^d\right)$ the Borel sigma algebra of $B^d$. Neglecting the constants, we have from $\mathrm{GRVaR}_D(\boldsymbol{X}) = \mathrm{GRVaR}_D(\boldsymbol{Y})$ that

$$\begin{aligned}
&\int_D \mathrm{VaR}_{\boldsymbol{u}}(\boldsymbol{X})\boldsymbol{\lambda}(\mathrm{d}\boldsymbol{u}) = \int_D \mathrm{VaR}_{\boldsymbol{u}}(\boldsymbol{Y})\boldsymbol{\lambda}(\mathrm{d}\boldsymbol{u}) \quad \forall D \in \mathscr{B}\left(B^d\right) \\
\Leftrightarrow &\int_D \mathrm{VaR}_{\boldsymbol{u}}(\boldsymbol{X}) - \mathrm{VaR}_{\boldsymbol{u}}(\boldsymbol{Y})\boldsymbol{\lambda}(\mathrm{d}\boldsymbol{u}) = 0 \quad \forall D \in \mathscr{B}\left(B^d\right),
\end{aligned}$$

which implies by a standard contradiction argument that $\mathrm{VaR}_{\boldsymbol{u}}(\boldsymbol{X}) - \mathrm{VaR}_{\boldsymbol{u}}(\boldsymbol{Y}) = 0$ for almost all $\boldsymbol{u} \in B^d$. Invoking Theorem 2.1 (4), we have $\boldsymbol{F}_X = \boldsymbol{F}_Y$. □

https://doi.org/10.1017/asb.2019.31 Published online by Cambridge University Press

Taken together, Propositions 5.1–5.4 show that GRVaR inherits the sensible behavior of geometric VaR regarding transformations and symmetries. Similarly to Theorem 2.1 in case of VaR, we summarize in Theorem 5.1 the properties of GRVaR established in Propositions 5.1–5.5 and Corollary 5.1.

**Theorem 5.1 (Properties of** GRVaR**).** *Denote by* $\boldsymbol{X} \in L^1(\Omega, \mathcal{F}, \mathbb{P})$ *a random vector and by* $D \subseteq \overline{B}^d$ *a fixed index vector set. Then*

*(1)* $\mathrm{GRVaR}_D(\boldsymbol{X} + \boldsymbol{x}) = \mathrm{GRVaR}_D(\boldsymbol{X}) + \boldsymbol{x}$ *for any vector* $\boldsymbol{x} \in \mathbb{R}^d$ *(translation invariance),*

*(2)* $\mathrm{GRVaR}_D(\sigma \boldsymbol{X}) = \sigma\, \mathrm{GRVaR}_D(\boldsymbol{X})$ *for any positive scalar* $\sigma > 0$ *(positive homogeneity),*

*(3)* $\mathrm{GRVaR}_{\widetilde{D}}(A\boldsymbol{X}) = A\, \mathrm{GRVaR}_D(\boldsymbol{X})$ *for any orthogonal matrix* $A \in \mathbb{R}^{d \times d}$*, where* $\widetilde{D} = A[D]$ *(rotation),*

*(4)* $\mathrm{GRVaR}_D(\boldsymbol{X}) = \mathrm{GRVaR}_D(\boldsymbol{Y})$ *for all measurable subsets* $D \subseteq B^d$ *if and only if* $\boldsymbol{F_X}(\boldsymbol{x}) = \boldsymbol{F_Y}(\boldsymbol{x})$ *for all* $\boldsymbol{x} \in \mathbb{R}^d$ *(distributional equality),*

*(5)* $\mathrm{GRVaR}_D(-\boldsymbol{X}) = -\,\mathrm{GRVaR}_{-D}(\boldsymbol{X})$ *(sign change) and*

*(6) if* $\boldsymbol{X}$ *is radially symmetric around* $\boldsymbol{\mu}$ *then* $\frac{1}{2}\big(\mathrm{GRVaR}_D(\boldsymbol{X}) + \mathrm{GRVaR}_{-D}(\boldsymbol{X})\big) = \boldsymbol{\mu}$ *(location symmetry).*

While Theorem 5.1 discusses the behavior of GRVaR for general index sets $D$, additional properties can be deduced for $D_+$ and $D_-$. As discussed at the end of Section 2, geometric quantiles asymptotically share the same direction as their underlying index. This especially implies that the signs of the components of $\mathrm{VaR}_{\alpha \boldsymbol{u}}(\boldsymbol{X})$ are equal to the sign of the components of $\boldsymbol{u}$, $\|\boldsymbol{u}\|_2 = 1$, when $\alpha \to 1$. Regarding GRVaR as an average over VaR, this implies in case of $D_+(\alpha_1, \alpha_2)$ that component-wise values of $\mathrm{GRVaR}_{D_+(\alpha_1,\alpha_2)}(\boldsymbol{X})$ eventually increase when $\alpha_2 \to 1$. The asymptotic growth rate of $\|\mathrm{VaR}_{\boldsymbol{\alpha}}(\boldsymbol{X})\|_2$ is known under moment conditions, see Girard and Stupfler (2017), and in a regular variation framework, see Girard and Stupfler (2015). In case of $D_-(\alpha_1, \alpha_2)$ it is not straightforward to parse out the component-wise behavior of $\mathrm{GRVaR}_{D_-(\alpha_1,\alpha_2)}(\boldsymbol{X})$ for $\alpha_2 \to 1$ since (asymptotically) the additional values gathered by increasing $\alpha_2$ are not all of the same sign. While the construction of $D_-(\alpha_1, \alpha_2)$ drops the orthant $O_-$ where all index components are negative, implying that for each index component there is one more orthant of positive values compared to negative ones, the precise effect on $\mathrm{GRVaR}_{D_-(\alpha_1,\alpha_2)}(\boldsymbol{X})$ cannot be directly determined and again depends on the growth rate of $\|\mathrm{VaR}_{\boldsymbol{\alpha}}(\boldsymbol{X})\|_2$ for $\boldsymbol{\alpha}$ in each orthant component of $D_-(\alpha_1, \alpha_2)$.

A similar effect holds when considering $\mathrm{GRVaR}_{D_+(\alpha,1)}(\boldsymbol{X})$ and $\mathrm{GRVaR}_{D_-(\alpha,1)}(\boldsymbol{X})$ for $\alpha$ close to one which is done in Section 6.3; see especially Figure 2. While the ordering with respect to $\alpha \in \{0.94, 0.95, 0.96\}$ in case of $D_+(\alpha, 1)$ is expected, Figure 2 shows that the same order also holds for $D_-(\alpha, 1)$ in this case.

https://doi.org/10.1017/asb.2019.31 Published online by Cambridge University Press

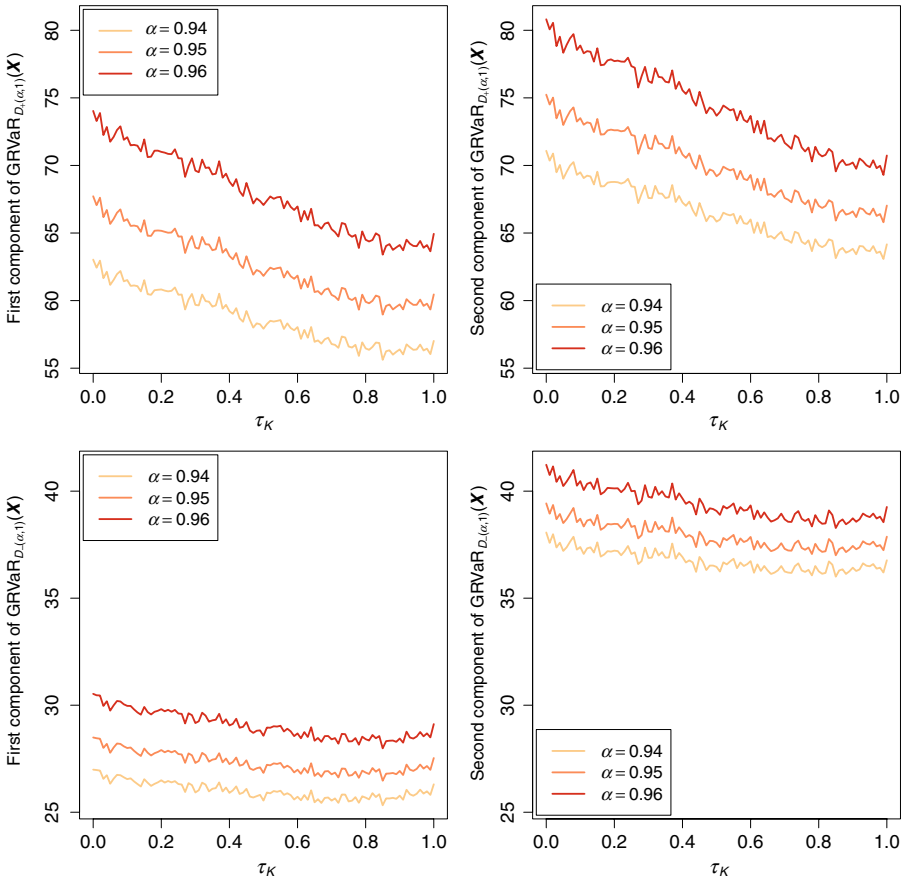



FIGURE 2: *Top*: First component (left) and second component (right) of $\mathrm{GRVaR}_{D_+(\alpha,1)}(\boldsymbol{X})$ for $\alpha \in \{0.94, 0.95, 0.96\}$. *Bottom*: First component (left) and second component (right) of $\mathrm{GRVaR}_{D_-(\alpha,1)}(\boldsymbol{X})$ for $\alpha \in \{0.94, 0.95, 0.96\}$. In all cases, the distribution of $\boldsymbol{X} = (X_1, X_2)$ has margins $X_i \sim \Gamma(i, 0.1)$ joined by a Clayton copula with Kendall's tau $\tau \in \{0, 0.01, 0.02, \ldots, 1\}$ and computations are based on 25,000 independent uniform draws from $D_+(\alpha, 1)$ and $D_-(\alpha, 1)$, and a sample size of 25,000 of the underlying joint distribution of $\boldsymbol{X}$.

## 6. ILLUSTRATION

In this section, we discuss special cases for which it is possible to obtain (semi-)closed-form expressions for GRVaR. Moreover, we provide numerical illustrations for a number of different random vectors in order to highlight the impact of changing margins and dependence structure, and compare multivariate GTVaR with univariate TVaR-based risk decomposition technique. This particular example is also used in order to provide corresponding indices when comparing GRVaR with univariate RVaR.

https://doi.org/10.1017/asb.2019.31 Published online by Cambridge University Press

### 6.1. Semi-closed-form solutions

A closed-form solution of GRVaR is only possible, if geometric VaR can be obtained explicitly. As a first candidate, we consider the bivariate uniform distribution on $[\boldsymbol{a}, \boldsymbol{b}] = [a_1, b_1] \times [a_2, b_2]$. In order to compute $\mathrm{VaR}_{\boldsymbol{\alpha}}(\boldsymbol{U})$ for a random vector $\boldsymbol{U} \sim \mathcal{U}([\boldsymbol{a}, \boldsymbol{b}])$, we compute

$$\begin{aligned}\mathbb{E}[\|\boldsymbol{U} - \boldsymbol{c}\|_2] &= \frac{1}{(b_1 - a_1)(b_2 - a_2)} \int_{a_1}^{b_1} \int_{a_2}^{b_2} \sqrt{(x - c_1)^2 + (y - c_2)^2}\, dy dx \\ &= \frac{1}{(b_1 - a_1)(b_2 - a_2)} \int_{a_1 - c_1}^{b_1 - c_1} \int_{a_2 - c_2}^{b_2 - c_2} \sqrt{x^2 + y^2}\, dy dx, \end{aligned} \tag{6.1}$$

where an integral transformation was used. Given two arbitrary constants $C_1$ and $C_2$, we introduce the auxiliary functions

$$h_1(x, y) = \frac{1}{2}\left(y \, \|(x, y)\|_2 + x^2 \log\left(y + \|(x, y)\|_2\right)\right) + C_1,$$

$$\begin{aligned} &h_2(x, y) \\ &= \frac{-x^3 + 6xy \, \|(x, y)\|_2 + 3y^3 \log\left(\|(x, y)\|_2 + x\right) + 3x^3 \log\left(\|(x, y)\|_2 + y\right)}{18} + C_2, \end{aligned}$$

where we have $\frac{d}{dx} h_2(x, y) = h_1(x, y)$ and $\frac{d}{dy} h_1(x, y) = \|(x, y)\|_2$. Using Fubini's theorem, the integration in (6.1) can thus be carried out as

$$\begin{aligned} &\mathbb{E}[\|\boldsymbol{U} - \boldsymbol{c}\|_2] \\ &= \frac{h_2(b_1 - c_1, b_2 - c_2) - h_2(a_1 - c_1, b_2 - c_2) - h_2(b_1 - c_1, a_2 - c_2) + h_2(a_1 - c_1, a_2 - c_2)}{(b_1 - a_1)(b_2 - a_2)}. \end{aligned}$$

Combining this with the univariate expectations $\mathbb{E}[U_i] = (b_i - a_i)/2$ leads to a closed-form solution of the objective function in (2.5). However, to actually compute VaR, the minimization in (2.5) still has to be carried out. This requires to take derivatives with respect to $c_1$ and $c_2$ which is intractable.

Aside from the uniform distribution, a distribution with independent normal margins leads to simplifications. We denote by $\boldsymbol{Z} \sim \mathcal{N}(\boldsymbol{\mu}, \boldsymbol{I}_d)$ a $d$-dimensional random vector with independent components which have possibly distinct means but unit variance. The norm $\chi = \|\boldsymbol{Z}\|_2$ of $\boldsymbol{Z}$ follows a noncentral chi distribution, and the density of $\chi$ follows directly from that of the noncentral chi-square distribution (see Johnson and Kotz, 1970, Chapter 28). The expectation of $\chi$ is essentially derived in Nuttal (1975, Equation (10)). After slight rearrangements, we have

$$\mathbb{E}[\chi^\beta] = \frac{2^{\frac{\beta}{2}} \Gamma\left(d/2 + \frac{\beta}{2}\right)}{\Gamma(d/2)} \mathbf{M}\left(-\frac{\beta}{2}; d/2; -\tfrac{1}{2}\|\boldsymbol{\mu}\|_2^2\right), \quad \beta > 0, \tag{6.2}$$

https://doi.org/10.1017/asb.2019.31 Published online by Cambridge University Press

where $\Gamma(x)$ denotes the gamma function and $\mathbf{M}(a;b;z)$ denotes the confluent hypergeometric function of the first kind, also known as Kummer's function. For the rising factorial $a^{(n)}$ with $a^{(0)}=1$ and $a^{(n)}=a(a+1)(a+2)\cdots(a+n-1)$, we have

$$\mathbf{M}(a;b;z)=\sum_{n=0}^{\infty}\frac{a^{(n)}z^n}{b^{(n)}n!}={}_1F_1(a;b;z).$$

$\mathbf{M}(a;b;z)$ is therefore a special case of the generalized hypergeometric function ${}_pF_q$; see Abramowitz and Stegun (1972).

Based on (6.2), the objective function in (2.3) can now be computed in closed form. For $\sigma>0$ and the random vector $\sigma\boldsymbol{Z}$ with $\boldsymbol{Z}$ as above, we have that

$$\begin{aligned}\mathbb{E}[\Phi_{\boldsymbol{\alpha}}(\sigma\boldsymbol{Z}-\boldsymbol{c})]&=\sigma\,\mathbb{E}[\Phi_{\boldsymbol{\alpha}}(\boldsymbol{Z}-\sigma^{-1}\boldsymbol{c})]=\sigma\,\mathbb{E}[\|\boldsymbol{Z}-\sigma^{-1}\boldsymbol{c}\|_2]+\sigma P_{\boldsymbol{\alpha}}(\sigma^{-1}\boldsymbol{c};\boldsymbol{Z})\\&=\sigma\frac{\sqrt{2}\Gamma\left(\frac{d+1}{2}\right)}{\Gamma(d/2)}\mathbf{M}\left(-\frac{1}{2};\frac{d}{2};-\frac{\|\boldsymbol{\mu}-\sigma^{-1}\boldsymbol{c}\|_2^2}{2}\right)+\sigma\sum_{i=1}^{d}\alpha_i(\mu_i-\sigma^{-1}c_i).\end{aligned}\tag{6.3}$$

With the derivative $\frac{d}{dz}\mathbf{M}(a;b;z)=\frac{a}{b}\mathbf{M}(a+1;b+1;z)$, see Equation 13.4.8 in Abramowitz and Stegun (1972), Equation (6.3) leads to an expression for the gradient $\nabla_{\boldsymbol{c}}\mathbb{E}[\Phi_{\boldsymbol{\alpha}}(\sigma\boldsymbol{Z}-\boldsymbol{c})]$. We then find $\mathrm{VaR}_{\boldsymbol{\alpha}}(\sigma\boldsymbol{Z})$ as the vector $\boldsymbol{c}$ for which $\nabla_{\boldsymbol{c}}\mathbb{E}[\Phi_{\boldsymbol{\alpha}}(\sigma\boldsymbol{Z}-\boldsymbol{c})]=\mathbf{0}$.

Similarly to the case of the uniform distribution, independent normal margins do not lead to a closed-form expression for geometric VaR, but a closed-form expression of the associated objective function. Given that closed-form solutions are hard to obtain, we consider numerical approximations next.

### 6.2. Numerical computation

While closed-form expressions for $\mathrm{GRVaR}_D(\boldsymbol{X})$ are hard to derive for a given random vector $\boldsymbol{X}$, we can use the conditional expectation formulation from Definition 3.1 to numerically compute $\mathrm{GRVaR}_D(\boldsymbol{X})$. Recalling $\boldsymbol{U}\sim\mathcal{U}(B^d)$, we can rewrite $\mathrm{GRVaR}_D(\boldsymbol{X})$ as

$$\mathrm{GRVaR}_D(\boldsymbol{X})=\mathbb{E}[\mathrm{VaR}_U(\boldsymbol{X})\mid\boldsymbol{U}\in D]=\frac{\mathbb{E}[\mathbb{1}_D(\boldsymbol{U})\,\mathrm{VaR}_U(\boldsymbol{X})]}{\mathbb{P}[\boldsymbol{U}\in D]}\tag{6.4}$$

$$\begin{aligned}&=\frac{1}{\lambda(D)/\lambda(B^d)}\int_D\mathrm{VaR}_{\boldsymbol{u}}(\boldsymbol{X})\frac{1}{\lambda(B^d)}\mathrm{d}\boldsymbol{u}\\&=\int_D\mathrm{VaR}_{\boldsymbol{u}}(\boldsymbol{X})\frac{1}{\lambda(D)}\mathrm{d}\boldsymbol{u}\\&=\mathbb{E}[\mathrm{VaR}_V(\boldsymbol{X})],\end{aligned}\tag{6.5}$$

where $\boldsymbol{V}$ is distributed uniformly on $D$, that is, $\boldsymbol{V}\sim\mathcal{U}(D)$. Equations (6.4) and (6.5) open up the possibility for numerical computations. To utilize either (6.4)

https://doi.org/10.1017/asb.2019.31 Published online by Cambridge University Press

or (6.5) in our setting, it is necessary to draw uniformly from either $B^d$ in case of (6.4), or $D_+$ and $D_-$ in case of (6.5). To this end, we provide the following algorithm which generalizes the well-known uniform sampling algorithms for balls; see, for example, Section 3.29 in Fishman (1996). An in-depth discussion of alternative sampling schemes for $B^d$ and the connections between them can be found in Harman and Lacko (2010).

**Algorithm 6.1.** Uniform distribution on $D(\alpha_1, \alpha_2)$

*To generate a pseudo-random vector* $\boldsymbol{U}$ *following a uniform distribution* $\mathcal{U}(D(\alpha_1, \alpha_2))$ *on* $D(\alpha_1, \alpha_2)$*, execute the following steps:*

(1) *Draw* $\boldsymbol{Y} = (Y_1, \ldots, Y_d)$*, where* $Y_i \sim \mathcal{N}(0, 1)$ *and all* $Y_i$ *are independent for* $i \in \{1, \ldots, d\}$.
(2) *Draw* $V \sim \mathcal{U}([0, 1])$.
(3) *Return* $\boldsymbol{U} = \left(\left(\alpha_2^d - \alpha_1^d\right) V + \alpha_1^d\right)^{1/d} \boldsymbol{Y} / \|\boldsymbol{Y}\|_2$.

It is clear that $\boldsymbol{Y}/\|\boldsymbol{Y}\|_2$ is distributed uniformly on the sphere and hence the distribution of $\boldsymbol{U}$ in Algorithm 6.1 is spherical in the sense of Fang *et al.* (1990, Chapter 2). Utilizing Fang *et al.* (1990, Theorem 2.9), it is further straightforward to show that the density of $\boldsymbol{U}$ is constant and hence uniform on $D(\alpha_1, \alpha_2)$. A formal argument for the uniformity of $\boldsymbol{U}$ on $D(\alpha_1, \alpha_2)$ is provided in the Appendix. By setting $\alpha_1 = 0$ and $\alpha_2 = 1$ the standard algorithm to sample from $B^d$ is recovered.

Reflections can further be used to obtain a uniform sample from $D(\alpha_1, \alpha_2)$ that is only contained in a given orthant $O_{\boldsymbol{s}}$; see (4.1). This finally allows to sample uniformly from $D_+$ and $D_-$.

**Proposition 6.1.** *Denote by* $\boldsymbol{U}$ *a random vector distributed uniformly on* $D(\alpha_1, \alpha_2)$*. For* $\boldsymbol{s} \in \{-1, 1\}^d$*, the random vector* $\boldsymbol{s}\,|\boldsymbol{U}| = (s_1\,|U_1|, \ldots, s_d\,|U_d|)$ *is then uniformly distributed on* $D(\alpha_1, \alpha_2) \cap O_{\boldsymbol{s}}$.

**Proof.** Without loss of generality, we show that $|\boldsymbol{U}| = (|U_1|, \ldots, |U_d|)$ is uniformly distributed on $D(\alpha_1, \alpha_2) \cap O_+$. First note that we have $\boldsymbol{\lambda}(D(\alpha_1, \alpha_2) \cap O_+) = \boldsymbol{\lambda}(D(\alpha_1, \alpha_2))/2^d$ by symmetry. To show that $|\boldsymbol{U}|$ is uniformly distributed on $D(\alpha_1, \alpha_2) \cap O_+$, we therefore have to show $\mathbb{P}[|\boldsymbol{U}| \in A] = \boldsymbol{\lambda}(A)/\boldsymbol{\lambda}(D(\alpha_1, \alpha_2) \cap O_+) = 2^d \boldsymbol{\lambda}(A)/\boldsymbol{\lambda}(D(\alpha_1, \alpha_2))$ for any set $A \subset D(\alpha_1, \alpha_2) \cap O_+$. Setting

$$\boldsymbol{s}A = \{\boldsymbol{x} \in \mathbb{R}^d \mid \boldsymbol{x} = (s_1 a_1, \ldots, s_d a_d), (a_1, \ldots, a_d) \in A\}$$

for $\boldsymbol{s} \in \{-1, 1\}^d$, we have

$$\begin{aligned}\mathbb{P}[|\boldsymbol{U}| \in A] &= \mathbb{P}[\boldsymbol{U} \in \cup_{\boldsymbol{s} \in \{-1,1\}^d} \boldsymbol{s}A] = \sum_{\boldsymbol{s} \in \{-1,1\}^d} \mathbb{P}[\boldsymbol{U} \in \boldsymbol{s}A] = \sum_{\boldsymbol{s} \in \{-1,1\}^d} \boldsymbol{\lambda}(\boldsymbol{s}A)/\boldsymbol{\lambda}(D(\alpha_1, \alpha_2)) \\ &= 2^d \boldsymbol{\lambda}(A)/\boldsymbol{\lambda}(D(\alpha_1, \alpha_2)),\end{aligned}$$

where the last equation follows from $\boldsymbol{\lambda}(\boldsymbol{s}_1 A) = \boldsymbol{\lambda}(\boldsymbol{s}_2 A)$ for $\boldsymbol{s}_1, \boldsymbol{s}_2 \in \{-1, 1\}^d$ since the Lebesgue measure is invariant under orthogonal transforms. □

https://doi.org/10.1017/asb.2019.31 Published online by Cambridge University Press

Numerical approximations based on (6.4) have the advantage that a global sampling algorithm on $B^d$ is sufficient to arrive at the approximations

$$\mathbb{E}[\mathbb{1}_D(\boldsymbol{U})\,\mathrm{VaR}_U(\boldsymbol{X})] \approx \frac{1}{M}\sum_{i=1}^{M} \mathbb{1}_D(\boldsymbol{u}_i)\,\mathrm{VaR}_{\boldsymbol{u}_i}(\boldsymbol{X}), \tag{6.6}$$

$$\mathbb{P}[\boldsymbol{U} \in D] \approx \frac{1}{M}\sum_{i=1}^{M} \mathbb{1}_D(\boldsymbol{u}_i), \tag{6.7}$$

where $(\boldsymbol{u}_i)_{i=1}^M$ is a sample of uniform pseudo-random vectors on $B^d$. While this strategy is applicable for any $D$, it features two distinct disadvantages. First, approximating $\mathbb{P}[\boldsymbol{U} \in D]$ via (6.7) in (6.4) leads to division by a random and possibly small quantity. Numerical errors in (6.7) can therefore destabilize the computation as a whole. Second, even if $\mathbb{P}[\boldsymbol{U} \in D]$ is known in closed form, as, for example, in case of $D_+$ and $D_-$, see (4.2), only roughly $\mu(D)$ sample points effectively contribute to the calculation of (6.6) due to the term $\mathbb{1}_D(\boldsymbol{u}_i)$. Whenever possible, we therefore suggest to rely on (6.5) for the numerical computation where we discuss the specific cases $D_+$ and $D_-$ next.

In contrast to the general applicability of (6.4), using (6.5) is only possible when a uniform sampling algorithm for $D$ is available. In this case however the resulting algorithm is more efficient since every observation contributes to the result and there is no division by a random quantity. For a sample $(\boldsymbol{v}_i)_{i=1}^M$ of pseudo-random vectors on $D$, the approximation is simply given by

$$\mathrm{GRVaR}_D(\boldsymbol{X}) \approx \frac{1}{M}\sum_{i=1}^{M} \mathrm{VaR}_{\boldsymbol{v}_i}(\boldsymbol{X}). \tag{6.8}$$

In case of $D_+$, we can directly apply (6.8) in conjunction with Algorithm 6.1 and Proposition 6.1 to obtain a uniform sample on $D_+$. In case of $D_-$, it is necessary to split the implied integration region $D$ in (6.5) as $D_- = \cup_{\substack{\boldsymbol{s}\in\{-1,1\}^d \\ \boldsymbol{s}\neq(-1,\dots,-1)}} D_{\boldsymbol{s}}$, where $D_{\boldsymbol{s}} = D(\alpha_1, \alpha_2) \cap O_{\boldsymbol{s}}$. With uniformly distributed random vectors $\boldsymbol{V}_{\boldsymbol{s}} \sim \mathcal{U}(D_{\boldsymbol{s}})$ and $\boldsymbol{U} \sim \mathcal{U}\left(B^d\right)$, we then have

$$\begin{aligned}
\mathrm{GRVaR}_{D_-}(\boldsymbol{X}) &= \frac{1}{\mathbb{P}[\boldsymbol{U} \in D_-]} \int_{B^d} \mathbb{1}_{D_-}(\boldsymbol{u})\,\mathrm{VaR}_{\boldsymbol{u}}(\boldsymbol{X}) \frac{1}{\lambda(B^d)}\mathrm{d}\boldsymbol{u} \\
&= \frac{1}{\lambda(D_-)/\lambda(B^d)} \sum_{\substack{\boldsymbol{s}\in\{-1,1\}^d \\ \boldsymbol{s}\neq(-1,\dots,-1)}} \int_{D_{\boldsymbol{s}}} \mathrm{VaR}_{\boldsymbol{u}}(\boldsymbol{X}) \frac{\lambda(D_{\boldsymbol{s}})}{\lambda(D_{\boldsymbol{s}})\lambda(B^d)}\mathrm{d}\boldsymbol{u} \\
&= \sum_{\substack{\boldsymbol{s}\in\{-1,1\}^d \\ \boldsymbol{s}\neq(-1,\dots,-1)}} \frac{\lambda(D_{\boldsymbol{s}})}{\lambda(D_-)} \mathbb{E}[\mathrm{VaR}_{\boldsymbol{V}_{\boldsymbol{s}}}(\boldsymbol{X})] \\
&= \frac{1}{2^d - 1} \sum_{\substack{\boldsymbol{s}\in\{-1,1\}^d \\ \boldsymbol{s}\neq(-1,\dots,-1)}} \mathbb{E}[\mathrm{VaR}_{\boldsymbol{V}_{\boldsymbol{s}}}(\boldsymbol{X})],
\end{aligned}$$

https://doi.org/10.1017/asb.2019.31 Published online by Cambridge University Press

where the last line follows since $\boldsymbol{\lambda}(D_-) = \frac{\pi^{d/2}(\alpha_2^d - \alpha_1^d)(2^d-1)}{\Gamma(d/2+1)2^d}$ and $\boldsymbol{\lambda}(D_s) = \frac{\pi^{d/2}(\alpha_2^d - \alpha_1^d)}{\Gamma(d/2+1)2^d}$ independently of $\boldsymbol{s}$. The individual expectations $\mathbb{E}[\mathrm{VaR}_{\nu_s}(\boldsymbol{X})]$ can now be approximated by sampling uniformly from $D_s$ via Algorithm 6.1 and Proposition 6.1.

All proposed approximations of course hinge on the possibility to compute geometric VaR, either in closed form or numerically. Aside from the discussion in Section 6.1, the numerical computation of geometric VaR via a Newton–Raphson-type iteration is discussed in Chaudhuri (1996). Alternatively, VaR can be computed by directly applying numerical minimization algorithms to an empirical version of (2.3). Also, in principle, (6.4) and (6.5) open the door for applying various variance-reduction techniques such as quasi-random numbers or importance sampling.

Alternatively to a random sampling strategy, nonrandom numerical integration schemes can be used to evaluate $\mathrm{GRVaR}_D(\boldsymbol{X})$. Quasi-random sampling is available in arbitrary dimensions and generally leads to a reduced variance compared to Monte Carlo sampling. For details on available error estimates and theory, see Lemieux (2009).

As an alternative, numerical integration techniques can be utilized. In this case, it is more suitable to integrate with respect to the Lebesgue measure $\boldsymbol{\lambda}$. In order to compute $\mathrm{GRVaR}_D(\boldsymbol{X})$, we are therefore forced to evaluate the integral

$$\frac{\Gamma(d/2+1)}{\pi^{d/2}\mu(D)} \int_D \mathrm{VaR}_{\boldsymbol{u}}(\boldsymbol{X}) \boldsymbol{\lambda}(d\boldsymbol{u});$$

see (3.5). We will focus on the integral involving $\mathrm{VaR}_{\boldsymbol{u}}(\boldsymbol{X})$, while leaving aside the implicit integral in $\mu(D)$. Numerical integration schemes are in most cases presented for a hyper-rectangular integration domain $\times_{i=1}^d [a_i, b_i]$ for $d = 2$ or $d = 3$. When $D$ is not of rectangular form, an appropriate coordinate transformation is therefore necessary to follow this approach. For example, for $d = 2$ the sets $D_+(\alpha_1, \alpha_2)$ and $D_-(\alpha_1, \alpha_2)$ can be represented in polar coordinates as

$$D_+(\alpha_1, \alpha_2) = \{(x, y) \in \mathbb{R}^2 : x = r\cos(\varphi), y = r\sin(\varphi), r \in [\alpha_1, \alpha_2], \varphi \in [0, \tfrac{1}{2}\pi]\},$$

$$D_-(\alpha_1, \alpha_2) = \{(x, y) \in \mathbb{R}^2 : x = r\cos(\varphi), y = r\sin(\varphi), r \in [\alpha_1, \alpha_2], \varphi \in [\tfrac{3}{2}\pi, 3\pi]\},$$

where the connected set $[\frac{3}{2}\pi, 3\pi]$ in case of $D_-$ is from a numerical point of view favorable compared to the unconnected set $[0, \pi] \cup [\frac{3}{2}\pi, 2\pi)$ linked to the standard parameterization $\varphi \in [0, 2\pi)$. Using integral transformation, the target integral for $D_+(\alpha_1, \alpha_2)$ can then be rewritten as

$$\begin{aligned} \int_{D_+(\alpha_1,\alpha_2)} \mathrm{VaR}_{(u_1,u_2)}(\boldsymbol{X}) du_1 du_2 &= \int_0^{\frac{1}{2}\pi} \int_{\alpha_1}^{\alpha_2} r\, \mathrm{VaR}_{(r\cos(\varphi), r\sin(\varphi))}(\boldsymbol{X}) dr d\varphi \\ &\approx \sum_{k=1}^{M} \beta_k r_k\, \mathrm{VaR}_{(r_k\cos(\varphi_k), r_k\sin(\varphi_k))}(\boldsymbol{X}), \end{aligned} \tag{6.9}$$

https://doi.org/10.1017/asb.2019.31 Published online by Cambridge University Press

where the node points $(r_k, \varphi_k)_{k=1}^M$ and weights $(\beta_k)_{k=1}^M$ are implied by the respective quadrature rule. Care has to be taken not to use a quadrature rule that places node points on the boundary $r = 1$ in case of GTVaR, since then geometric VaR is undefined. One example of an integration rule that does not place node points on the boundary is Gaussian quadrature; see Stoer and Bulirsch (2002) for details and a general introduction to numerical quadrature.

### 6.3. Numerical illustrations

One can interpret multivariate geometric risk measures as a risk decomposition technique embedded in an aggregate risk measure, since one computes allocated amounts based on a formula which aggregates risks. In this application, we compare multivariate GTVaR with a TVaR-based risk decomposition technique, where the expectation of each one of the random variables is calculated, conditional on the aggregation of all dependent risks. For more details on the TVaR-based risk decomposition technique, we refer the reader to Cossette *et al.* (2012) and references therein.

Consider a bivariate portfolio $S = X_1 + X_2$, where each $X_i$ follows a Gamma distribution with parameters $(\gamma_i, \beta)$, where $\gamma_i = i$ and $\beta = 0.1$ for $i \in \{1, 2\}$ such that $\mathbb{E}[X_1] = 10$ and $\mathbb{E}[X_2] = 20$. Moreover, assume a dependence structure represented by a Clayton copula, with dependence parameter $\theta$. In the independence case ($\theta = 0$), we can easily obtain $F_S^{-1}(0.99) = 84.06025$, $\mathrm{TVaR}_{0.99}(S) = 96.38035$, which can be analytically decomposed into amounts allocated for each $X_i$, $i = 1, 2$, that is, $\mathrm{TVaR}_{0.99}(X_1;S) = 32.12678$ and $\mathrm{TVaR}_{0.99}(X_2;S) = 64.25357$, where $\mathrm{TVaR}_\kappa(X_i;S) = E[X_i | S > \mathrm{VaR}_\kappa(S)]$, $i = 1, 2$; see Cossette *et al.* (2012) for details. Then, using a positive dependence structure between $X_1$ and $X_2$ represented by $\theta = 1.2$, we have $F_S^{-1}(0.99) = 90.09976$, $\mathrm{TVaR}_{0.99}(S) = 102.74714$, which can be analytically decomposed into amounts allocated for each $X_i$, $i = 1, 2$, that is, $\mathrm{TVaR}_{0.99}(X_1;S) = 37.21703$ and $\mathrm{TVaR}_{0.99}(X_2;S) = 65.53011$.

We now turn toward a comparison of GRVaR and the TVaR decomposition of Cossette *et al.* (2012) outlined above. To do so, we consider GRVaR based on four index sets that all extend to the boundary of $B^d$ and hence GRVaR can be interpreted as geometric TVaR in this case. For $0 \leqslant \alpha < 1$, we consider the introduced sets $D_-(\alpha, 1)$ and $D_+(\alpha, 1)$. To add one additional degree of freedom, we also consider rotations of $D_-(\alpha, 1)$ and $D_+(\alpha, 1)$ around the origin. For $\varphi \in [0, 2\pi)$, the rotation can be accomplished by multiplying an element $\boldsymbol{u}$ of an index set by a rotation matrix

$$R_\varphi = \begin{pmatrix} \cos(\varphi) & -\sin(\varphi) \\ \sin(\varphi) & \cos(\varphi) \end{pmatrix},$$

leading to the rotated index sets $R_\varphi D_-(\alpha, 1)$ and $R_\varphi D_+(\alpha, 1)$. The rotated index set naturally combines with the properties of GRVaR, especially Proposition 5.3. For a given vector $\boldsymbol{c} = (c_1, c_2)$, we then proceed to find

https://doi.org/10.1017/asb.2019.31 Published online by Cambridge University Press

TABLE 1

VALUES OF $\alpha_{\pm}^{*}$ AND $(\alpha_{\pm}^{*}, \varphi_{\pm}^{*})$ SUCH THAT THE RESULTING GRVaR BASED ON $D_{\pm}(\alpha_{\pm}^{*}, 1)$ OR $R_{\varphi_{\pm}^{*}} D_{\pm}(\alpha_{\pm}^{*}, 1)$ IS CLOSE TO $\boldsymbol{c}_1 = (32.12678, 64.25357)$ (FOR $\theta = 0$) AND $\boldsymbol{c}_2 = (37.21703, 65.53011)$ (FOR $\theta = 1.2$) IN EUCLIDEAN DISTANCE.

| Specification | $\theta = 0$ | $\theta = 1.2$ |
|---|---|---|
| $\alpha_{+}^{*}$ | 0.8374934 | 0.8798641 |
| $\mathrm{GRVaR}_{D_{+}(\alpha_{+}^{*},1)}(\boldsymbol{X})$ | (42.76010, 52.55561) | (46.22415, 55.38499) |
| $\alpha_{-}^{*}$ | 0.9855055 | 0.9902669 |
| $\mathrm{GRVaR}_{D_{-}(\alpha_{-}^{*},1)}(\boldsymbol{X})$ | (42.64916, 52.07197) | (46.40202, 54.56433) |
| $(\alpha_{+}^{*}, \varphi_{+}^{*})$ | (0.8678664, 0.3381556) | (0.8962714, 0.2598723) |
| $\mathrm{GRVaR}_{R_{\varphi_{+}^{*}} D_{+}(\alpha_{+}^{*},1)}(\boldsymbol{X})$ | (32.12678, 64.25357) | (37.21699, 65.53013) |
| $(\alpha_{-}^{*}, \varphi_{-}^{*})$ | (0.9891655, 5.066231) | (0.9920267, 4.977593) |
| $\mathrm{GRVaR}_{R_{\varphi_{-}^{*}} D_{-}(\alpha_{-}^{*},1)}(\boldsymbol{X})$ | (32.12706, 64.25359) | (37.21715, 65.53020) |

Computations of GRVaR are based on a sample size of 20,000 of the underlying joint distribution of $\boldsymbol{X}$ and a two-dimensional Gauss–Legendre product quadrature scheme with $50^2$ node points as outlined in (6.9), where the integration domains are $[\alpha_{+}^{*}, 1] \times [\varphi_{+}^{*}, \varphi_{+}^{*} + \pi/2]$ and $[\alpha_{-}^{*}, 1] \times [\varphi_{-}^{*}, \varphi_{-}^{*} + 3\pi/2]$ in case of bivariate optimization. Optimal values are found via a derivative free Nelder–Mead optimization method.

the values of $\alpha$ or $(\alpha, \varphi)$ that minimize the Euclidean distance between the geometric TVaR of $\boldsymbol{X} = (X_1, X_2)$ and $\boldsymbol{c}$ via

$$\alpha_{\pm}^{*} = \operatorname*{argmin}_{\alpha \in [0,1]} \left\| \mathrm{GRVaR}_{D_{\pm}(\alpha,1)}(\boldsymbol{X}) - \boldsymbol{c} \right\|_2, \quad \text{or}$$

$$(\alpha_{\pm}^{*}, \varphi_{\pm}^{*}) = \operatorname*{argmin}_{(\alpha,\varphi) \in [0,1] \times [0,2\pi]} \left\| \mathrm{GRVaR}_{R_{\varphi} D_{\pm}(\alpha,1)}(\boldsymbol{X}) - \boldsymbol{c} \right\|_2.$$

Based on the TVaR decomposition of Cossette *et al.* (2012), we use $\boldsymbol{c}_1 = (32.12678, 64.25357)$ in case of independence, while for positive dependence we use $\boldsymbol{c}_2 = (37.21703, 65.53011)$.

The results are reported in Table 1. We see that with a single free parameter it is not possible to find an index $\alpha_{\pm}^{*}$ that yields a close fit. The standard domains $D_{+}(\alpha, 1)$ and $D_{-}(\alpha, 1)$, which are motivated by theoretical considerations, do therefore not lead to very close fits. When allowing for additional rotation, the two parameter models on the other hand yield very close numerical values in all cases, which highlights the versatility of the suggested approach. However, we do not consider this an intrinsic shortcoming of the suggested domains $D_{+}$ and $D_{-}$. Instead of trying to reproduce the risk decomposition exactly, these index sets are motivated to complete the picture of the risk inherent in $\boldsymbol{X}$ when combined with other approaches. Furthermore, we use this example to exemplify the difficulty of comparing parameter values across different generalizations of multivariate TVaR that are designed for different circumstances.

To get a better understanding of the behavior of geometric GTVaR, we consider, for the same marginal setup, changes in the underlying dependence

https://doi.org/10.1017/asb.2019.31 Published online by Cambridge University Press

structure. To cover the full range of possible parameter values for $\theta$ in $[0, \infty)$, we parameterize the Clayton copula via Kendall's tau. For the Clayton copula, Kendall's tau is given as $\tau_K = \theta/(\theta + 2)$ and we consider values of $\tau_K$ in the grid $[0, 0.01, 0.02, \ldots, 1]$, where the limiting case $\tau_K = 1$ leads to a comonotonic dependence structure. For a better comparison, we compute $\mathrm{GRVaR}_{D_+(\alpha,1)}$ and $\mathrm{GRVaR}_{D_-(\alpha,1)}$ for different levels $\alpha \in \{0.94, 0.95, 0.96\}$. Figure 2 shows in the top row the first and second components for $\mathrm{GRVaR}_{D_+(\alpha,1)}$, while the bottom row shows the first and second components for $\mathrm{GRVaR}_{D_-(\alpha,1)}$. It is interesting to see that larger values of $\tau_K$ lead overall to smaller values of the components of $\mathrm{GRVaR}_{D_+(\alpha,1)}$ and $\mathrm{GRVaR}_{D_-(\alpha,1)}$. Modulo the inherent randomness in the sample and the calculations, this decrease seems to be monotonic in terms of $\tau_K$. This also fits with the observation that in case of the comonotonic limit ($\tau_K = 1$), one of the lowest component-wise values is attained. At the same time, the curves are ordered in accordance to the values of $\alpha$. While the curves generally decrease as a function of $\tau_K$, this effect is more pronounced for the index set $D_+(\alpha, 1)$ compared to $D_-(\alpha, 1)$. The fact that the values of the first component are for both index sets lower than those of the second fits with the fact that the mean and variance of the first margin are lower than those of the second margin in the given example. For the Gamma distribution $\Gamma(\gamma, \beta)$ with density $x \mapsto f_\Gamma(x;\gamma, \beta)$ and quantile function $p \mapsto F_\Gamma^{-1}(p;\gamma, \beta)$, the TVaR is given as

$$\mathrm{TVaR}_\alpha(X) = \frac{\gamma\left(1 - f_\Gamma\left(F_\Gamma^{-1}(\alpha;\gamma,\beta);\gamma+1,\beta\right)\right)}{\beta(1-\alpha)}, \quad X \sim \Gamma(\gamma,\beta).$$

In terms of the marginal TVaR, we therefore have for the first component $\mathrm{TVaR}_{0.94}(X_1) = 38.13411$, $\mathrm{TVaR}_{0.95}(X_1) = 39.95732$ and $\mathrm{TVaR}_{0.96}(X_1) = 42.18876$, while we have for the second component $\mathrm{TVaR}_{0.94}(X_2) = 57.03272$, $\mathrm{TVaR}_{0.95}(X_2) = 59.17963$ and $\mathrm{TVaR}_{0.96}(X_2) = 61.79073$. Comparing the marginal values with the component-wise values of GRVaR reported in Figure 2, we see that GRVaR based on $D_+(\alpha, 1)$ results in higher component-wise values regardless of the strength of dependence measured in $\tau_K$. On the other hand, the index set $D_-(\alpha, 1)$ leads uniformly to lower component-wise values.

To better understand the relationship to the univariate TVaR, we consider an alternative representation. Recalling (3.1) for the first component of $\boldsymbol{X} = (X_1, X_2)$ with $U \sim \mathcal{U}([0, 1])$ and $\alpha \in (0, 1)$,

$$\mathrm{TVaR}_\alpha(X_1) = \frac{1}{1-\alpha}\int_\alpha^1 F_{X_1}^{-1}(u)du = \mathbb{E}\left[F_{X_1}^{-1}(U) \mid U \geqslant \alpha\right],$$

we can in the same spirit integrate the first component of the bivariate geometric value-at-risk $\mathrm{VaR}_{\boldsymbol{\alpha}}(\boldsymbol{X}) = \left(\mathrm{VaR}_{\boldsymbol{\alpha}}^1(\boldsymbol{X}), \mathrm{VaR}_{\boldsymbol{\alpha}}^2(\boldsymbol{X})\right)$. This requires adjusting the confidence level from $(0, 1)$ to $(-1, 1)$ via $\widetilde{\alpha} = 2\alpha - 1$. Comparable to the univariate case, we can now integrate the first component of geometric VaR

https://doi.org/10.1017/asb.2019.31 Published online by Cambridge University Press

$$\frac{1}{1-\widetilde{\alpha}}\int_{\widetilde{\alpha}}^{1}\mathrm{VaR}^{1}_{(u,0)}(\boldsymbol{X})du=\mathbb{E}\left[\mathrm{VaR}^{1}_{(\widetilde{U},0)}(\boldsymbol{X})\mid\widetilde{U}\geqslant\widetilde{\alpha}\right]$$
$$=\frac{1}{2(1-\alpha)}\int_{2\alpha-1}^{1}\mathrm{VaR}^{1}_{(u,0)}(\boldsymbol{X})du, \tag{6.10}$$

where $\widetilde{U}\sim\mathcal{U}([-1,1])$. The index $(u,0)$ is comparable to the univariate confidence level since it is aligned with the first coordinate axes. A comparison of $\mathrm{VaR}^{1}_{(u,0)}(\boldsymbol{X})$ and $\mathrm{VaR}_u(X_1)$ can be found in Herrmann *et al.* (2018). The connection between (6.10) and geometric GTVaR can be seen when considering the marginal and conditional distributions of a random vector that is uniformly distributed on $B^2$. When $\boldsymbol{U}=(U_1,U_2)$ is uniformly distributed on $B^2$, the marginal distributions are given by the Wigner semicircle distribution with density

$$f_{U_i}(u)=\frac{2}{\pi}\sqrt{1-u^2}\mathbb{1}_{[-1,1]}(u),\qquad i\in\{1,2\}.$$

The marginal density given $U_2=u_2$ is however uniform on $\left[-\sqrt{1-u_2^2},\sqrt{1-u_2^2}\right]$, specifically we have

$$f_{U_1|U_2}(u_1|u_2)=\frac{1}{2\sqrt{1-u_2^2}}\mathbb{1}_{\left[-\sqrt{1-u_2^2},\sqrt{1-u_2^2}\right]}(u_1).$$

For $U_2=0$, the distribution of $U_1\mid U_2=0$ is hence uniform on $[-1,1]$. When denoting this conditional random variable by $\widetilde{U}$, that is,

$$\widetilde{U}\;=\;U_1\mid U_2=0\;\sim\;\mathcal{U}([-1,1]),$$

we have that

$$\mathbb{E}\left[\mathrm{VaR}^{1}_{(\widetilde{U},0)}(\boldsymbol{X})\mid\widetilde{U}\geqslant\widetilde{\alpha}\right]=\mathbb{E}\left[\mathrm{VaR}^{1}_{U}(\boldsymbol{X})\mid\boldsymbol{U}\in D(\alpha)\right], \tag{6.11}$$

where $D(\alpha)=\{(x,0)\in\mathbb{R}^2|2\alpha-1\leqslant x\leqslant 1\}=\{(x,0)\in\mathbb{R}^2\mid\widetilde{\alpha}\leqslant x\leqslant 1\}$. The right-hand side of (6.11) is the first component of $\mathrm{GRVaR}_{D(\alpha)}$. This shows that comparing (3.1) to (6.10) falls into our framework when considering the specific set $D(\alpha)$.

In Figure 3, we compare the two approaches visually for the previously considered joint distributions with gamma margins and a Clayton copula. To this end, we introduce four two-dimensional random vectors $\boldsymbol{X}_i=(X_{i1},X_{i2})$, $i\in\{1,2,3,4\}$. The first margins $X_{i1}$, $i\in\{1,2,3,4\}$, have parameters $(\gamma,\beta)=(1,0.1)$, while the second margins $X_{i2}$, $i\in\{1,2,3,4\}$, have parameters $(\gamma,\beta)=(2,0.1)$. In case of $\boldsymbol{X}_1$, both components are independent, while the margins of $\boldsymbol{X}_2$ are joined by a Clayton copula with parameter $\theta=1.2$. For $\boldsymbol{X}_3$ we consider the comonotonic copula, while $\boldsymbol{X}_4$ follows the counter monotonic copula model. Both copulas fit into our discussion as they are limiting cases of the Clayton copula model; see Nelsen (2006, Chapter 4.2). Figure 3 shows the

https://doi.org/10.1017/asb.2019.31 Published online by Cambridge University Press

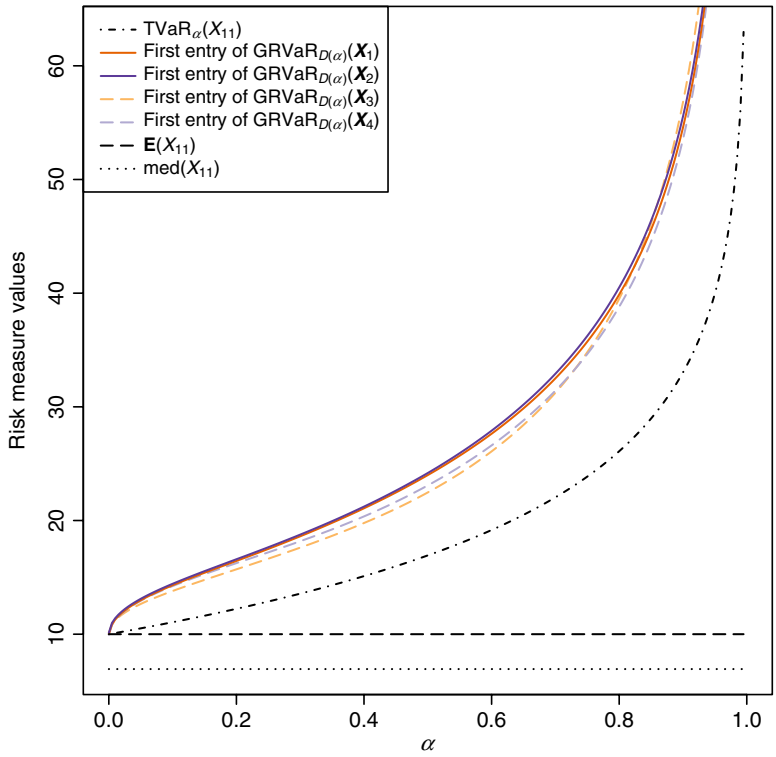



FIGURE 3: TVaR$_\alpha(X_{11})$ for $\alpha \in [0, 0.005, \ldots, 0.995]$ (dotted-dashed). First component of GRVaR$_{D(\alpha)}(\boldsymbol{X}_1)$ (orange, solid), GRVaR$_{D(\alpha)}(\boldsymbol{X}_2)$ (violet, solid), GRVaR$_{D(\alpha)}(\boldsymbol{X}_3)$ (light orange, dashed) and GRVaR$_{D(\alpha)}(\boldsymbol{X}_4)$ (light violet, dashed). Numerical integration of (6.10) via Gauss–Legendre quadrature with 45 node points. Each value of geometric VaR based on 15,000 pseudo-random draws from $\boldsymbol{X}_i$, $i \in \{1, 2, 3, 4\}$. Mean (dashed) and median (dotted) of $X_{11}$ in black.

resulting univariate TVaR$_\alpha(X_{11})$ (which is equivalent to TVaR$_\alpha(X_{i1})$ for $i \in \{2, 3, 4\}$) in black (dotted-dashed line), while the first entries of GRVaR$_{D(\alpha)}(\boldsymbol{X}_1)$ and GRVaR$_{D(\alpha)}(\boldsymbol{X}_2)$ are given in orange and violet (solid lines). The first entries of GRVaR$_{D(\alpha)}(\boldsymbol{X}_3)$ and GRVaR$_{D(\alpha)}(\boldsymbol{X}_4)$ are given in light orange and light violet (dashed lines). While TVaR$_\alpha(X_{11})$ can be computed in closed form, the integral in (6.10) used to compute the first entry of GRVaR$_{D(\alpha)}(\boldsymbol{X}_i)$, $i \in \{1, 2, 3, 4\}$, is numerically evaluated by Gauss–Legendre quadrature with 45 node points. In this case, the integrand given by geometric VaR is numerically computed based on 15,000 pseudo-random draws from $\boldsymbol{X}_i$. For reference, the mean and median of $X_{11}$ are shown in dashed and dotted black lines. As shown in Figure 3, the first component of GRVaR$_{D(\alpha)}(\boldsymbol{X}_i)$, $i \in \{1, 2\}$, is higher than TVaR$_\alpha(X_1)$ for the considered $\alpha \in [0, 0.005, \ldots, 0.995]$. Furthermore, the dependence present between the components of $\boldsymbol{X}_2$ leads to higher values of GRVaR$_{D(\alpha)}(\boldsymbol{X}_2)$ compared to GRVaR$_{D(\alpha)}(\boldsymbol{X}_1)$. It is interesting to note that GRVaR$_{D(\alpha)}(\boldsymbol{X}_3)$ and GRVaR$_{D(\alpha)}(\boldsymbol{X}_4)$ eventually form an envelope for GRVaR$_{D(\alpha)}(\boldsymbol{X}_1)$ and GRVaR$_{D(\alpha)}(\boldsymbol{X}_2)$ when $\alpha$ is large enough. While we have

https://doi.org/10.1017/asb.2019.31 Published online by Cambridge University Press

for large values of $\alpha$ the intuitively expected order where higher values of association between $X_{i1}$ and $X_{i2}$ lead to higher risk measure values, this is not the case for lower values of $\alpha$ where the comonotonic dependence structure yields the lowest risk measure values.

In all cases, we numerically recover $\mathrm{GRVaR}_{D(0)}(\boldsymbol{X}_i) = \mathbb{E}[X_1]$, $i \in \{1, 2, 3, 4\}$. While this is in line with our expectations from the univariate theory, it remains an open problem to formally show the following two equalities:

$$\mathrm{GRVaR}_{D(0)}(\boldsymbol{X}) = \mathbb{E}[X_1],$$
$$\mathrm{GRVaR}_{B^d}(\boldsymbol{X}) = \mathbb{E}[\boldsymbol{X}] = (\mathbb{E}[X_1], \ldots, \mathbb{E}[X_d]).$$

Both equalities generalize $\mathrm{TVaR}_0(X) = \mathbb{E}[X]$ to the multivariate case by maximizing the considered index set and are numerically verified for the considered examples.

## 7. Conclusion

We defined multivariate versions of TVaR and RVaR. Our generalizations were based on the geometric quantiles introduced in Chaudhuri (1996) for which we derived a previously unknown symmetry property; see Theorem 2.1 (6). Comparable to the univariate case, GRVaR is defined in terms of a conditional expectation of geometric VaR for extreme index vectors. In case of geometric VaR, the index vectors are $d$-variate vectors that replace the customary univariate confidence levels, leading (in general) to a multivariate conditioning set. We discussed the construction of index sets which are suitable to capture extreme index vectors in the multivariate case and identified two index sets that capture either component-wise or jointly extreme risks which we studied in detail. Furthermore, geometric GTVaR and GRVaR are shown to be well-behaved under the most common transformations such as translation, scaling and reordering. They are also shown to inherit previously derived symmetry properties from the underlying geometric quantiles.

We also discussed possible avenues of computing geometric GTVaR and GRVaR. Aside from semi-closed-form solutions for special cases, we discussed Monte Carlo simulation techniques for our functionals and compared them numerically to risk decomposition techniques for sums of random variables. The Monte Carlo computation of GRVaR is facilitated by a new uniform sampling scheme for rings and their intersection with orthants that generalizes known sampling schemes for the unit ball. Compared to the risk decomposition technique of Cossette *et al.* (2012), the indices used for geometric GTVaR are substantially different. This highlights the need for further investigation of the interpretation of the indices. Furthermore, increasing the positive dependence in the considered Clayton copula-based model leads to a slight decrease in the component values.

In order to compare geometric GTVaR to univariate TVaR, we also studied the difference between univariate TVaR and the first component of geometric

https://doi.org/10.1017/asb.2019.31 Published online by Cambridge University Press

GTVaR for a suitable index set. For the considered models, geometric GTVaR based on this index set is higher than the comparable univariate TVaR. For high confidence levels, the geometric GTVaR values are furthermore ordered with higher values of the parameter of the underlying Clayton copula, that is, stronger dependence in the sense of concordance. While higher values of the parameter lead to higher values of the first component of geometric GTVaR, the mean is recovered as a special case when the integration set is maximized as expected from the univariate case. We leave other possible multivariate expected-shortfall-type generalizations discussed in Section 3 and the open problems discussed at the end of Section 6 for further research.

## Acknowledgments

This work was supported by NSERC under Grant nos. RGPIN-5010-2015 and RGPIN-2015-05447.

## References

Abramowitz, M. and Stegun, I. (1972) *Handbook of Mathematical Functions with Formulas, Graphs, and Mathematical Tables*, 10th. Mineola: Dover Publications.

Artzner, P., Delbaen, F., Eber, J.M. and Heath, D. (1999) Coherent measures of risk. *Mathematical Finance*, **9**(3), 203–228.

Ben Tahar, I. (2006) Tail conditional expectation for vector-valued risks. *SFB 649 Discussion Papers*.

Chaudhuri, P. (1996) On a geometric notion of quantiles for multivariate data. *Journal of the American Statistical Assosiation*, **91**(434), 862–872.

Cherubini, U., Luciano, E. and Vecchiato, W. (2004) *Copula Methods in Finance*. Hoboken: John Wiley & Sons.

Cont, R., Deguest, R. and Scandolo, G. (2010) Robustness and sensitivity analysis of risk measurement procedures. *Quantitative Finance*, **10**(6), 593–606.

Cossette, H., Mailhot, M. and Marceau, É. (2012) TVaR-based capital allocation for multivariate compound distributions with positive continuous claim amounts. *Insurance: Mathematics and Economics*, **50**(2), 247–256.

Cossette, H., Mailhot, M., Marceau, É. and Mesfioui, M. (2013) Bivariate lower and upper orthant value-at-risk. *European Actuarial Journal*, **3**(2), 321–357.

Cossette, H., Mailhot, M., Marceau, É. and Mesfioui, M. (2016) Vector-valued tail value-at-risk and capital allocation. *Methodology and Computing in Applied Probability*, **18**(3), 653–674.

Di Bernardino, E., Fernández-Ponce, J.M., Palacios-Rodríguez, F. and Rodríguez-Griñolo, M.R. (2015) On multivariate extensions of the conditional value-at-risk measure. *Insurance: Mathematics and Economics*, **61**, 1–16.

Di Bernardino, E., Laloë, T., Maume-Deschamps, V. and Prieur, C. (2013) Plug-in estimation of level sets in a non-compact setting with applications in multivariable risk theory. *ESAIM: Probability and Statistics*, **17**, 236–256.

Embrechts, P. and Puccetti, G. (2006) Bounds for functions of multivariate risks. *Journal of Multivariate Analysis*, **97**(2), 526–547.

Fang, K.T., Kotz, S. and Ng, K.W. (1990) *Symmetric Multivariate and Related Distributions*. London: Chapman & Hall.

Fishman, G. (1996) *Monte Carlo: Concepts, Algorithms, and Applications*, Springer.

Girard, S. and Stupfler, G. (2015) Extreme geometric quantiles in a multivariate regular variation framework. *Extremes*, **18**, 629–663.

https://doi.org/10.1017/asb.2019.31 Published online by Cambridge University Press

GIRARD, S. and STUPFLER, G. (2017) Intriguing properties of extreme geometric quantiles. *Revstat*, **15**, 107–139.
HARMAN, R. and LACKO, V. (2010) On decompositional algorithms for uniform sampling from n-spheres and n-balls. *Journal of Multivariate Analysis*, **101**, 2297–2304.
HERRMANN, K., HOFERT, M. and MAILHOT, M. (2018) Multivariate geometric expectiles. *Scandinavian Actuarial Journal*, **7**, 629–659.
JOHNSON, N.L. and KOTZ, S. (1970) *Continuous Univariate Distributions - 2*, 1st edition. Boston: Houghton Mifflin Company.
KAAS, R., GOOVAERTS, M., DHAENE, J. and DENUIT, M. (2008) *Modern Actuarial Risk Theory*, 2nd edition. New York: Springer.
KIM, J. and HARDY, M. (2009) A capital allocation based on a solvency exchange option. *Insurance: Mathematics and Economics*, **44**(3), 357–366.
KOENKER, R. and BASSETT, J.R. (1978) Regression quantiles. *Econometrica*, **46**(1), 33–50.
KOLTCHINSKII, V.I. (1997) M-estimation, convexity and quantiles. *Annals of Statistics*, **25**(2), 435–477.
LEMIEUX, C. (2009) *Monte Carlo and Quasi-Monte Carlo Sampling*, New York: Springer-Verlag.
MAUME-DESCHAMPS, V., RULLIÈRE, D. and SAID, K. (2017) Multivariate extensions of expectiles risk measures. *Dependence Modeling*, **5**(1), 20–44.
MCNEIL, A., FREY, R. and EMBRECHTS, P. (2015) *Quantitative Risk Management: Concepts, Techniques, and Tools*, 2nd edition. Princeton: Princeton University Press.
NELSEN, R.B. (2006) *An Introduction to Copulas*, New York: Springer-Verlag.
NEWEY, W. and POWELL, J. (1987) Asymmetric least squares estimation and testing. *Econometrica*, **55**(4), 819–847.
NUTTAL, A.H. (1975) Some integrals involving the $Q_M$ function. *IEEE Transactions on Information Theory*, **21**(1), 95–96.
RUBIN, L., RANSON, N. and SHI, X. (2009) Analysis of Methods for Determining Margins for Uncertainty under a Principle-Based Framework for Life Insurance and Annuity Products. *Society of Actuaries*, March.
SMALL, C. (1990) A survey of multidimensional medians. *International statistical review*, **58**(3), 263–277.
STOER, J. and BULIRSCH, R. (2002) *Introduction to Numerical Analysis*, 3rd edition. New York: Springer.

KLAUS HERRMANN (Corresponding author)
*Department of Statistics and Actuarial Science*
*University of Waterloo*
*Waterloo, Ontario, Canada*
*E-Mail: klaus.herrmann@uwaterloo.ca*

MARIUS HOFERT
*Department of Statistics and Actuarial Science*
*University of Waterloo*
*Waterloo, Ontario, Canada*
*E-Mail: marius.hofert@uwaterloo.ca*

MÉLINA MAILHOT
*Department of Mathematics and Statistics*
*Concordia University*
*Montréal, Québec, Canada*
*E-Mail: melina.mailhot@concordia.ca*

https://doi.org/10.1017/asb.2019.31 Published online by Cambridge University Press

# APPENDIX: UNIFORM DISTRIBUTION ON $D(\alpha_1, \alpha_2)$

Denote by $\boldsymbol{Y} = (Y_1, \dots, Y_d)$, $Y_i \sim \mathcal{N}(0,1)$ a vector of mutually independent standard normals and by $V \sim \mathcal{U}([0,1])$ a standard uniform random variable independent of $\boldsymbol{Y}$. Then the random vector $\boldsymbol{U} = \left(\left(\alpha_2^d - \alpha_1^d\right)V + \alpha_1^d\right)^{1/d} \boldsymbol{Y}/\|\boldsymbol{Y}\|_2$ follows a spherical distribution, where the random vector $\boldsymbol{Y}/\|\boldsymbol{Y}\|_2$ is uniformly distributed on the sphere and $R = \left(\left(\alpha_2^d - \alpha_1^d\right)V + \alpha_1^d\right)^{1/d}$ is the corresponding radial part with distribution and density function

$$\boldsymbol{F}_R(u) = \begin{cases} 0, & \text{for } u < \alpha_1, \\ \frac{u^d - \alpha_1^d}{\alpha_2^d - \alpha_1^d}, & \text{for } \alpha_1 \leqslant u \leqslant \alpha_2, \\ 1, & \text{for } u > \alpha_2. \end{cases} \qquad f_R(u) = \begin{cases} \frac{du^{d-1}}{\alpha_2^d - \alpha_1^d}, & \text{for } \alpha_1 \leqslant u \leqslant \alpha_2, \\ 0, & \text{otherwise.} \end{cases}$$

By Fang *et al.* (1990, Theorem 2.9), this implies that $\boldsymbol{U}$ has a density, where the density generator $g$ fulfills

$$\frac{du^{d-1}}{\alpha_2^d - \alpha_1^d} = \frac{2\pi^{d/2} u^{d-1}}{\Gamma(d/2)} g(u^2).$$

Using $f_{\boldsymbol{U}}(\boldsymbol{x}) = g\left(\|\boldsymbol{x}\|_2^2\right)$ and $d\Gamma(d/2)/2 = \Gamma(d/2+1)$, the density of $\boldsymbol{U}$ is then given as

$$f_{\boldsymbol{U}}(\boldsymbol{x}) = \frac{\Gamma(d/2+1)}{\pi^{d/2}\left(\alpha_2^d - \alpha_1^d\right)},$$

which is the normalization of the Lebesgue measure of $D(\alpha_1, \alpha_2)$ implying that $\boldsymbol{U}$ is uniformly distributed.

https://doi.org/10.1017/asb.2019.31 Published online by Cambridge University Press